THESIS

STRENGTHENING FOR PRE-TENSION BRIDGE GIRDER BY LINK SLAB

OLARN WIENGWEERA

GRADUATE SCHOOL, KASETSART UNIVERSITY
2008

THESIS APPROVAL

GRADUATE SCHOOL, KASETSART UNIVERSITY

Master of Engineering (Civil Engineering)
DEGREE

Civil Engineering	Civil Engineering
FIELD	**DEPARTMENT**

TITLE: Strengthening for Pre-tension Bridge Girder by Link Slab

NAME: Mr. Olarn Wiengweera

THIS THESIS HAS BEEN ACCEPTED BY

THESIS ADVISOR
(Associate Professor Prasert Suwanvitaya, Ph.D.)

Trakool Aramraks **COMMITTEE MEMBER**
(Associate Professor Trakool Aramraks, Ph.D.)

Wiwat Seangthien **COMMITTEE MEMBER**
(Mr. Wiwat Seangthien, Ph.D.)

DEPARTMENT HEAD
(Associate Professor Korchoke Chantawarangul, Ph.D.)

APPROVED BY THE GRADUATE SCHOOL ON 30 May 2008

Gunjana Theeragool **DEAN**
(Associate Professor Gunjana Theeragool, D.Agr.)

THESIS

STRENGTHENING FOR PRE-TENSION BRIDGE GIRDER BY LINK SLAB

OLARN WIENGWEERA

A Thesis Submitted in Partial Fulfillment of
the Requirements for the Degree of
Master of Engineering (Civil Engineering)
Graduate School, Kasetsart University
2008

Olarn Wiengweera 2008: Strengthening for Pre-tension Bridge Girder by Link Slab. Master of Engineering (Civil Engineering), Major Field: Civil Engineering, Department of Civil Engineering. Thesis Advisor: Associate Professor Prasert Suwanvitaya, Ph.D. 79 pages.

Trucks have recently been allowed to carry greater load than previous limits. Existing bridges are getting older, while the traffic has increased in response to transportation demand. The need for strengthening of highway bridges was considered for maintenance cost efficiency and service life. The strengthening of bridge superstructure by link slab is a retrofit method for changing the behavior from simple span to continuous span of multi-simple-span bridge. By this method, tension reinforcement in the deck is essential to resist the negative moment at connecting region. This thesis aims to study and investigate the behaviour and load carrying capacity of a joint of adjoining beams continuously made by the link slab.

In the experiment, two precast concrete beams were joined as one simple beam with cast-in-place reinforced concrete deck. The gap between the two precast concrete beams was filled with non-shrinkage mortar. Two different sizes of link slab beams were tested under two point loading system to compare with monolithic beams. The results of this study showed that the flexure capacity of both link slab beams was about the same as the corresponding conventional beams.

Student's signature Thesis Advisor's signature 30/May/08

ACKNOWLEDGEMENT

The author would like to express his profound gratitude to his advisor, Assoc. Prof. Dr. Prasert Suwanvitaya for his guidance and invaluable advice throughout the period of this research. And also to Assoc. Prof. Dr. Trakool Aramraks, Assoc. Prof. Dr. Korchoke Chantawarangul, and Dr. Wiwat Saengthien for their comments and suggestions in this research.

Sincere appreciation is also extended to Dr. Chakree Bamrungwong for his useful advice, and many persons who participated and helped in preparation of specimens and testing. Particular, thanks is given to Sika (Thailand) Limited for supporting non – shrinkage material used in this study.

Finally, the author would like to extend grateful thanks to his parents and friends who have continuously given support of all kinds and inspiration.

Olarn Wiengweera
April 2008

TABLE OF CONTENTS

LIST OF TABLES

LIST OF FIGURES

LIST OF FIGURES (Continued)

Appendix Figure **Page**

LIST OF FIGURES (Continued)

Figure **Page**

LIST OF ABBREVIATIONS

a	=	Depth of equivalent rectangular stress block
As	=	Area of reinforcement, $cm.^2$
A'_s	=	Area of compression reinforcement, $cm.^2$
A_v	=	Area of shear reinforcement within a distance s
b	=	Width of compression face of member, cm.
b_v	=	Width of cross section at contact surface being investigated for horizontal shear, cm.
C	=	Compressive force in cross section, kg subscripts c = concrete, s = steel
c	=	Distance from extreme compression fiber to neutral axis
DB	=	Deformed bar
d	=	Distance from extreme compression fiber to centroid of tension reinforcement, cm.
E_c	=	Modulus of elasticity of concrete, ksc
E_s	=	Modulus of elasticity of reinforcement, ksc
f'_c	=	Specified compressive strength of concrete, ksc.
f_v	=	Modulus of rupture of concrete, ksc.
f_s	=	Calculated stress in reinforcement at service loads, ksc.
f_y	=	Specified yield strength of reinforcement, ksc.
h	=	Overall depth of member, $cm.^2$
I_{cv}	=	Moment of inertia of cracked section transformed to concrete, $cm.^4$
I_g	=	Moment of inertia of gross concrete section about centroidal axis, neglecting reinforcement, $cm.^4$
k	=	Effective length factor for compression members
L	=	Span length, m.
M_{cr}	=	Computed moment capacity, kg-m.
M_n	=	Cracking moment, kg-m.

LIST OF ABBREVIATIONS (Continued)

n	=	Point load
P	=	Nominal moment strength of a section
RB	=	Rounded bar
T	=	Tensile force in cross section, kg.
s	=	Spacing of shear reinforcement in direction parallel to the longitudinal reinforcement
V	=	Design shear force at section
r	=	Design shear stress at section
V_c	=	Nominal shear strength provided by concrete
r_c	=	Permissible shear stress carried by concrete
r_h	=	Permissible horizontal shear stress
V_n	=	Nominal shear strength
V_{nh}	=	Nominal horizontal shear strength
V_s	=	Nominal shear strength provided by shear reinforcement
y_t	=	Distance from centroidal axis of gross section, neglecting reinforcement, to extreme fiber in tension
$\beta 1$	=	Ratio of depth of rectangular stress block, a, to depth of neutral axis, c
ρ	=	Tension reinforcement ratio = As / bd
ρb	=	Reinforcement ratio producing balanced strain conditions
ε_{cu}	=	Compressive strain at crushing of concrete
ε_s	=	Strain in steel
$\varnothing$	=	Diameter
θ	=	Rotation angle

STRENGTHENING FOR PRE-TENSION BRIDGE GIRDER BY LINK SLAB

INTRODUCTION

There have been prestressed concrete bridges in Thailand since 1960s. Prestressed concrete girders were fabricated in various spans from 5 to 60 meters. Most waterway bridges were built by the Department of Highways (D.O.H.), the Public Works Department (P.W.D), and the Department of Accelerated Rural Development (D.A.R.D.). The last two departments later merged to form the Department of Rural Roads (D.R.R.) in 2002 under the Ministry of Transport and Communications (M.T.C). Prestressed concrete simple span bridges are popular because it has been proven they are economical and time – effective. Prestressed concrete girders have been prefabricated in the forms of pre-tensioned plank girder, box girder. Detail of typical plank and box girder are shown in Appendix A, spanning 5 to 20 meters, and I girder span 20 to 50 meters, fabricated in both pre – tensioning and post – tensioning system. In the past, design of bridges used the requirements according to Standard Specifications for Highway Bridges by the American Association of State Highway and Transportation Officials (AASHTO). The highway live loadings on the roadway of bridge consist of standard truck or lane load class HS 20-44 (Appendix B). Such live loading was generated forces (moment and shear) covering Thai trucks in the beginning through to the trucks with promulgated in 1993 (D.O.H; P.W.D.; D.A.R.D; 1993)

The heavier trucks have constantly been developed to carry more load. The Ministry of Transport and Communication has recently allowed trucks to carry greater load than previous limits. Consequently, live load for bridge design has been changed to 1.3 of HS 20-44 (P.W.D., 1999). New truck weight limits which were promulgated in 2006 (Appendix B) cause the forces (moment and shear) to exceed the ideal truck, HS 20-44 (Appendix B, Table 1). Existing bridges are adversely affected by the new limits. Although the overloading does not cause immediate collapse of bridges, it is expected that bridges will deteriorate faster, have shorter service life, and in general, increase maintenance cost. Several methods were introduced to retrofit the old bridges for durability under consideration of their performance.

Table 1 Moment at mid span and end shear for load lane of simple span due to live loadings

Loading	Span 10 m.		Span 20 m.	
	Moment (kg.- m.)	Shear (kg.)	Moment (kg.- m.)	Shear (kg.)
HS 20-44 Truck	42,420	23,362	124,067	28,010
HS 20-44 Lane	32,318	16,556	88,449	21,319
Truck 1	45,350	21,070	108,500	26,418
Truck 2	45,350	22,790	119,250	28,248
Semi-trailer 1	47,625	24,400	152,875	34,987
Semi-trailer 2	52,063	22,058	130,350	34,667
Full trailer 1	54,775	25,780	158,874	33,607
Full trailer 2	54,775	25,780	166,849	35,155
Full trailer 3	53,750	23,895	152,825	34,862

Strengthening of a bridge by link slab is a method to make a simple span bridge carry more load . Link slab changes a simple span as shown in Figure 1(a) to be a continuous span as shown in Figure 1(b) by putting tensile reinforcing steel at the joint of two adjacent spans to resist the negative moment at the joint on pier or bent.

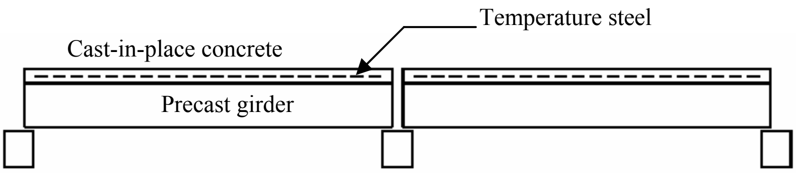

a. Conventional simple span

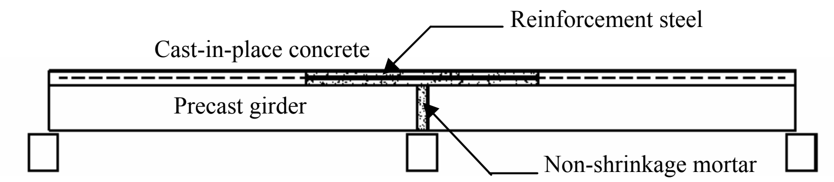

b. Continuity by link slab

Figure 1 Strengthening by link slab

Strengthening of pre–tension bridge girder or multi–beam by link slab is an easy method for such a superstructure. The procedure can be performed on precast girder without formwork or shoring; furthermore, the traffic can still pass in case of bridges with two lanes or more.

OBJECTIVES

The objectives of this study are:

1. To determine the flexural behavior of the beams connected by link slab method.

2. To propose model to explain link slab behavior.

Scope of Research

1. Use reinforced concrete beam as the precast concrete beam.

2. The specimens' ultimate load capacity was calculated.

3. Two kinds of composite beams, monolithic beam versus link slab beam were studied.

4. For each kind, two cross-sections were studied.

5. Each beam was subjected to two points loading until failure.

LITERATURE REVIEW

Jointless bridges have been built since the 1930's using design and construction procedures developed from the success of field prototypes. Research in jointless bridge deck construction aims to accomplish four design objectives: (1) Long–term serviceability, (2) minimal maintenance requirements, (3) economical construction and (4) improved overall performance. (Larson , 2005)

Several methods for providing continuity in prestressed concrete construction have been applied in practice. Continuous beams may be divided into two classes : fully continuous beams and partially continuous beams. For partial continuity, each span can be precast as a simple beam, using sufficient amount of prestressed steel for handling and erection. Generally, no falsework is required for erection. Concrete at the support section is cast–in–place after the precast beams are erected. Several possible details are show in Figure 2, for such partially continuous beams.

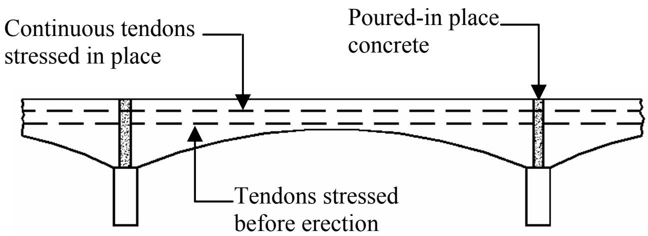

a. Continuous tendons stressed after erection

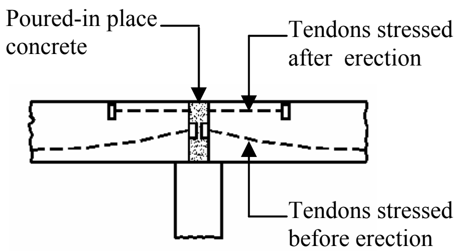

b. Short tendons stressed over support

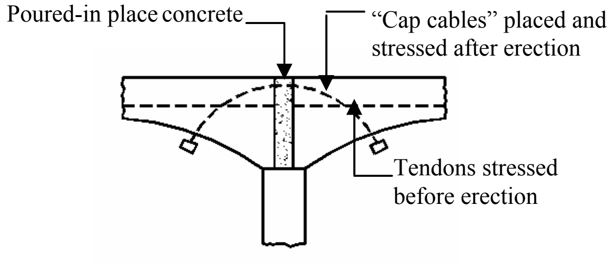

c. Cap cables over supports

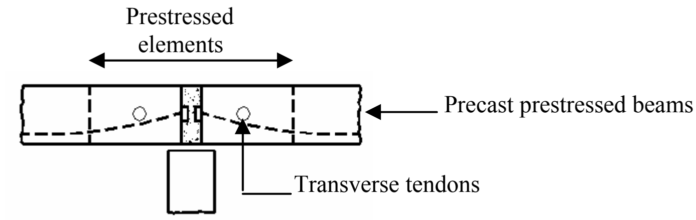

d. Continuous element over supports transversely prestressed

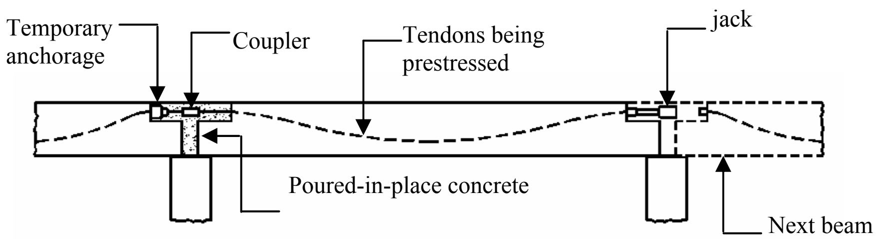

e. Continuous elements over supports transversely prestressed

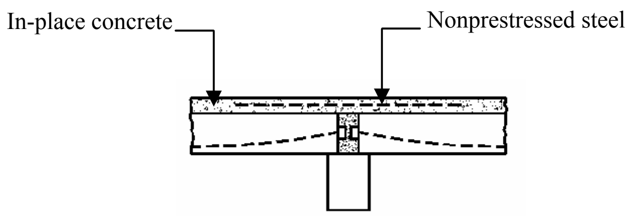

f. Nonprestressed steel over supports

Figure 2 Layouts for partially continuous beams

Source: LIN and BURNS (1980)

The section of the deck connecting the two adjacent simple span girders is called the link slab. Figure 2 (f) shows continuity of simple span beams by link slab. Precast elements can be conveniently made continuous for live load by placing nonprestressed steel over the support. This is especially true for composite construction where a topping concrete is poured in place. Propping of the precast elements will be required prior to casting the composite slab. The sequence of construction for a bridge structure using this detail is shown in Figure 3 below:

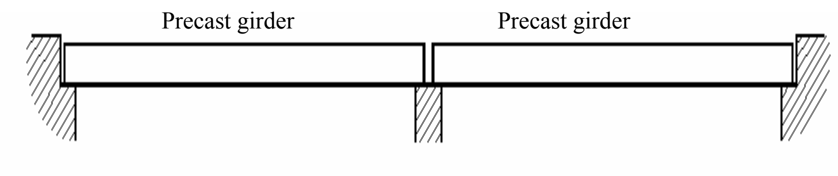

Stage 1 Precast girders in place

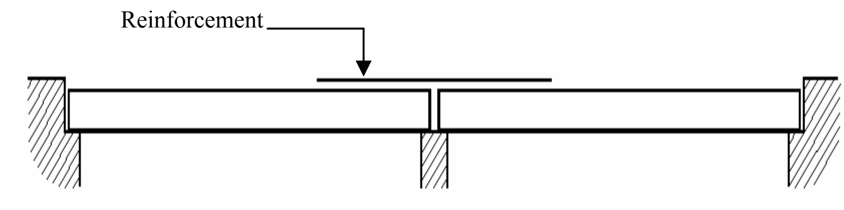

Stage 2 Reinforcement at support

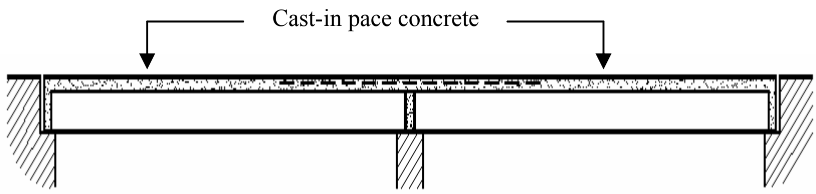

Stage 3 Completed structure

Figure 3 Sequence of construction for continuity by link slab
Source: LIN and BURNS (1980)

The real behavior of jointless bridges is extremely complex because of the development of secondary forces due to the movements induced by temperature, creep, and shrinkage. Despite these complexities we know that jointless bridges perform satisfactorily. (Henry and Lee,1994) However, Burke (1993) indicated that for bridge lengths less thon 300 ft (90 m), bridge spans less than 80 fit (24 m.), and skews less than 30 degree or curvatures less than 5 deg, many of these secondary factors should be neglected.

Caner and Zia (1998) experimentally analyzed the performance of jointless bridge decks and proposed design methods for the link slab. These investigations revealed that the link slab was subjected to bending under typical traffic conditions rather than axial elongation. Tensile cracks were observed at the top of the link slab under service conditions due to a negative bending moment. They pointed out that additional tensile stress may be imposed on the link slabs due to shrinkage, creep, and temperature loading, and that crack width must be carefully controlled. The recommendation was to use epoxy coated reinforcing bars in the link slab in order to avoid reinforcement corrosion. To reduce the stiffness of the link slab, debonding of the link slab over the girder joint for a length equal to 5% of each girder span was also recommended. This link slab concept can be used for new bridge decks and also for replacement of deteriorated joints of existing bridge decks.

The design concept for a reinforced concrete link slab with two identical adjacent spans outlined in Caner and Zia (1998) will be summarized in the following.

Step 1 Determine end rotation angle of spans θ

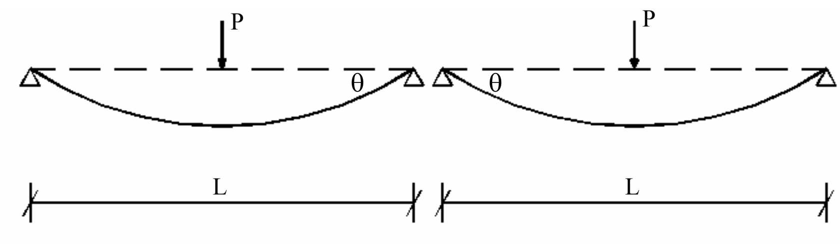

Figure 4 Simplified geometry and loading of two-span bridge structure

The rotation angle θ is a function of the geometry of the spans, their loading, and material properties. Assuming both spans are simply supply supported, the rotation angle can be derived as:

$$\theta = \frac{PL_{sp}^2}{16E_c I_{sp}}$$

Step 2 Determine moment of inertia of link slab (uncracked)

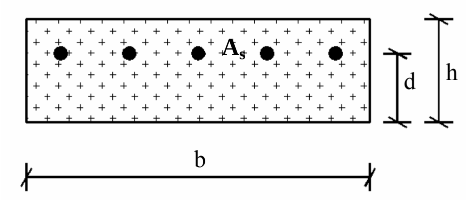

Figure 5 Cross-sectional dimensions and reinforcement of link slab in uncracked condition

The moment of inertia of the link slab in the uncracked conditions is a function of the cross-sectional geometry and independent of the reinforcement ratio $\rho = A_s / B_{ls}H_{ls}$

$$I_{ls,g} = \frac{B_{ls}H_{ls}^3}{12}$$

Step 3 Determine moment M_a developed in the link slab at rotation angle θ

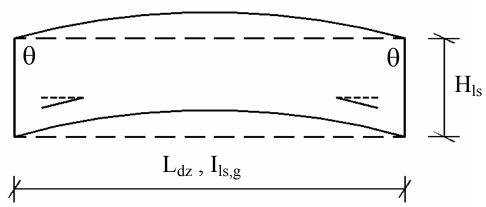

Figure 6 Deformed shape of link slab at imposed rotation angle θ

The moment developed in the uncracked link slab is a function of the material properties and geometrical dimensions. It is proportional to the imposed rotation angle θ

$$M_a = \frac{2E_c I_{ls,g}}{L_{dz}}\theta$$

Step 4 Determine cracking moment M_{cr} in link slab

The cracking moment M_{cr} is a function of the first cracking strength of the cementitious material used in this particular link slab with given geometry.

$$M_{cr} = \frac{\delta_{cr} I_{ls,g}}{\frac{H_{ls}}{2}} = \delta_{cr} \frac{B_{ls} H_{ls}^2}{6}$$

Compare applied moment M_a to cracking moment M_{cr}.

Step 5 Select reasonable longitudinal reinforcement ratio $\rho = 0.01$ H_{ls}

Step 6 Determine cracked moment of inertia I_{cr}

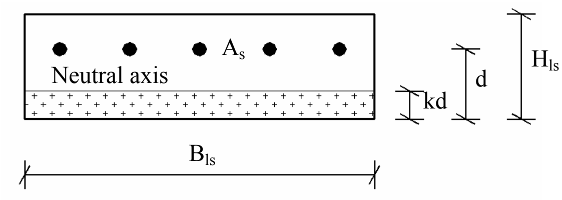

Figure 7 Cross-sectional dimensions and reinforcement of link slab in cracked condition

The cracked moment of inertia results from contributions of the uncracked portion below the neutral axis, of the reinforcement itself, and from the eccentricity of the reinforcement with respect to the neutral axis. With $n = \frac{E_s}{E_c}$, and $k = -n\rho + \sqrt{(n\rho)^2 + 2(n\rho)}$, follows

$$I_{ls,cr} = \frac{B_{ls}(kd)^3}{12} + B_{ls}kd\left(\frac{kd}{2}\right)^2 + nA_s(d-kd)^2$$

$$= \frac{B_{ls}(kd)^3}{3} + nA_s(d-kd)^2$$

The cracked moment of inertia is a function of the cross-sectional dimensions as well as of the reinforcement ratio ρ. Assuming a fixed position of the neutral axis and elastic material behavior, it will remain constant at increasing rotation angles θ.

Step 7 Determine stress in longitudinal reinforcement σ_s and compare with allowable stress $0.40\ \sigma_y$

The stress in the link slab reinforcement σ_s as derived in Caner and Zia (1998) is expressed as:

$$\sigma_s = \frac{M_a}{M_{cr}} \frac{\sigma_{cr}}{6\rho\gamma^2\left(1+\frac{1}{3}\left(n\rho-\sqrt{(n\rho)^2+2n\rho}\right)\right)}$$

This expression indicates a dependency of the stress in the reinforcement on the ratio of applied moment M_a to the cracking moment of the link slab M_{cr}. However, with $\gamma = \frac{d}{H_{ls}}$ follows

$$\sigma_s = \frac{M_a}{M_{cr}} \frac{\sigma_{cr}}{6\frac{A_s}{\gamma B_{ls}H_{ls}}\left(\frac{d}{H_{ls}}\right)^2\left(1-\frac{1}{3}k\right)} = \frac{M_a}{\cancel{M_{cr}}} \frac{\cancel{\sigma_{cr}}\frac{\cancel{B_{ls}}H_{ls}^2}{6}}{A_s\left(d-\frac{1}{3}kd\right)}$$

$$= \frac{M_a}{A_s\left(d-\frac{1}{3}kd\right)} = \frac{\frac{2E_c I_{ls,g}}{L_{dz}}\theta}{A_s\left(d-\frac{1}{3}kd\right)} \le 0.40\sigma_y$$

Step 8 Check surface crack width criterion ($W < W_{max}$)

Besides the stress limit state described above, the current design procedure also limits the maximum crack width at the top of the link slab. The expected crack width is a function of the stress in the reinforcement as determined in Step 7 as well as a function of the geometry of the link slab. The following expression has been adopted from Gergely and Lutz (1968).

$W = 0.076\beta\sigma_s\sqrt[3]{d_c A}[0.001in]$, with $\beta = \frac{H_{ls}-kd}{H_{ls}-d}$

In addition to the crack width criterion adopted in this design guideline (Caner and Zia, 1998), FHWA recommends a minimum reinforcement ratio ρ=0.015 with a clear cover of 2.5 in for the purpose of controlling the crack width in the link slab.

Theoretical Background and Computation Model

Behavior of Continuous- span Bridge

A continuous span is advantageous over a simple span in carrying increased flexure, or on the other hand, continuity enables structure to carry more load. Because continuity causes distribution of moment from the mid span to the connection on the intermediate support, the positive moment occurs less compared with simple span. Figure 8 shows HS20-44, AASHTO standard truck, which is the typical moving load used in design or analysis of bridge move along two simple-spans bridge 20 m. length and continuous two spans bridge 40 m. length. The positive bending moments shown in Figure 9 indicate that for the same loading and span length, the continuous-span bridge occurs positive moment as 78% of the simple-span bridge at mid span.

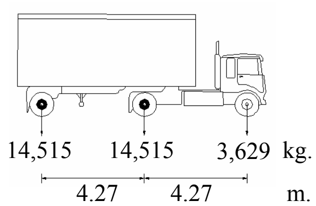

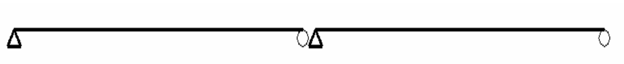

a. Simple-span bridge

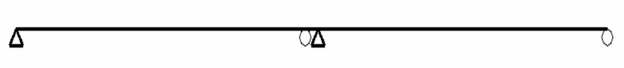

b. Continuous-span bridge

Figure 8 AASHTO standard truck and two types of bridges

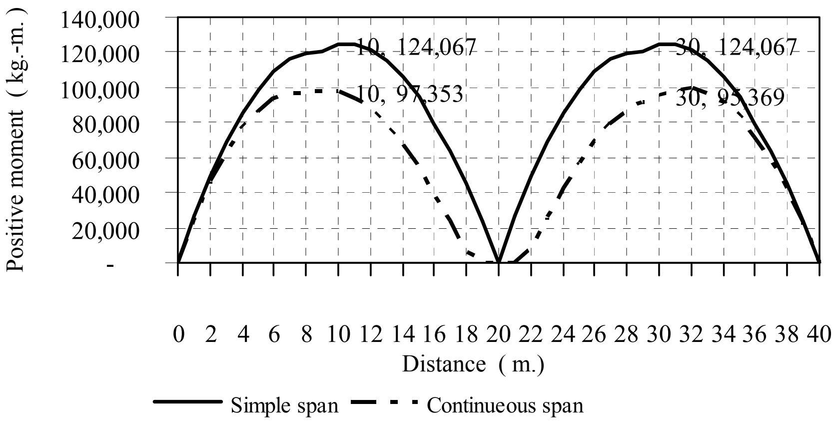

Figure 9 Comparison of positive moment of simple and continuous span bridge due to HS20-44 truck loading

From Figure 9, it can be seen that the moment ratio of simple to continuous span at mid span equals 1.27. Although a continuous-span bridge benefits in reduction positive moment, the characteristic of continuous span, it also generates negative moment affecting capability of connection. Figure 10 shows moment in the continuous-span bridge due to 1.27 times of HS20-44 truck loading. Such a negative moment needs significant consideration in retrofit of a simple-span bridge to be a continuous-span bridge.

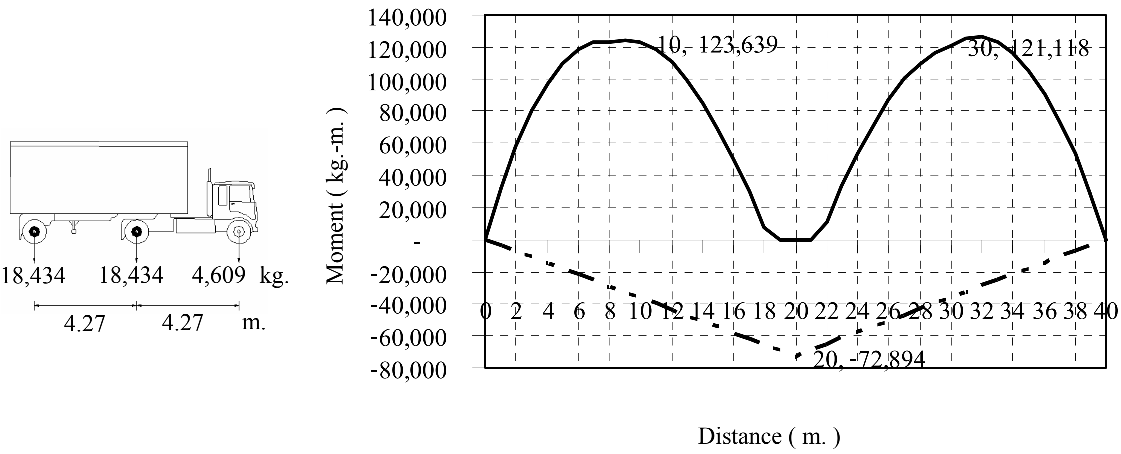

Figure 10 Moment in continuous-span bridge due to 1.27 times of HS20-44 truck loading

Design of Reinforced Concrete for Negative Moment

Basic Assumptions in Flexure Theory

Three basic assumptions are made:

1. Sections perpendicular to the axis of bending which are plane before bending remain plane after bending.

2. The strain in the reinforcement is equal to the strain in the concrete at the same level.

3. The stresses in the concrete and reinforcement can be computed from the strains using stress-strain curves for concrete and steel.

Additional assumptions in flexure theory for design:

4. The tensile strength of concrete is neglected in flexural strength calculations.

5. Concrete is assumed to fail when the compressive strain reaches a limiting value.

Analysis of Reinforced Concrete Beam by Strength Method

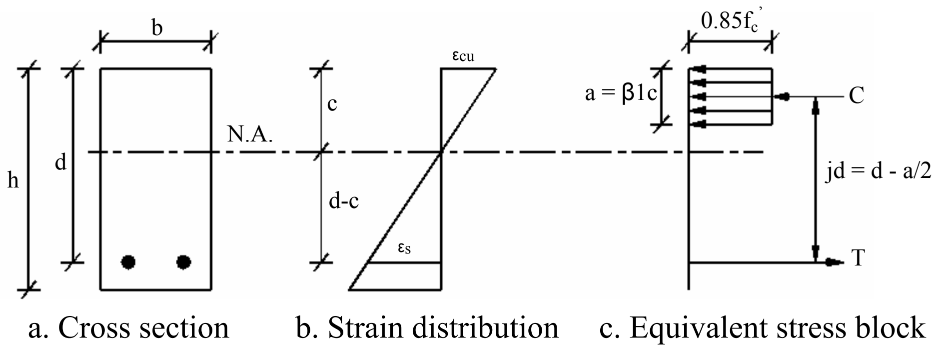

Figure 11 Analysis of rectangular beam with tension reinforcement only

Consider the beam shown in Fig.9, compressive force in the concrete is:

$$C = 0.85 f_c^{'} ba$$

Then tension force in the steel is

$$T = A_s f_y$$

and for equilibrium, C = T . Therefore, the depth, a, is :

$$a = \frac{A_s f_s}{0.85 f_c^{'} b}$$

If tension steel yielded, $f_s = f_y$, then

$$a = \frac{A_s f_y}{0.85 f_c^{'} b}$$

Determination of whether $f_s = f_y$

Consider the strain distribution shown in Fig.9, from similar triangle:

$$\frac{c}{d} = \frac{\varepsilon_{cu}}{\varepsilon_{cu} + \varepsilon_s}$$

where $c = \dfrac{a}{\beta_1}$

$$\beta_1 = \begin{cases} 0.85 & ; \quad f_c^{'} \le 280 ksc. \\ 0.85 - 0.05\left(\dfrac{f_c^{'} - 280}{70}\right) & ; \quad 280 < f_c^{'} < 560 ksc. \\ 0.65 & ; \quad f_c^{'} > 560 ksc. \end{cases}$$

Substitute $\varepsilon_{cu} = 0.003$; then

$$\frac{c}{d} = \frac{0.003}{0.003 - \varepsilon_s}$$

$$\varepsilon_s = 0.003\left(\frac{d-c}{c}\right)$$

If $\varepsilon_s > \varepsilon_y, \left(\varepsilon_y = \dfrac{f_y}{E_s}\right)$, the beam is tension controlled.

The nominal moment capacity; $M_n = Tjd$

$$M_n = A_s f_y \left(d - \frac{a}{2}\right)$$

The flexural cracking moment ; $$M_{cr} = \frac{f_r I_g}{y_t}$$

Where $f_r = 1.98\sqrt{f_c^{'}}$

Calculation of Deflection

When a concrete beam is loaded, it undergoes a deflection referred to as an immediate deflection, Δ_i, determination of an immediate deflection as follows:

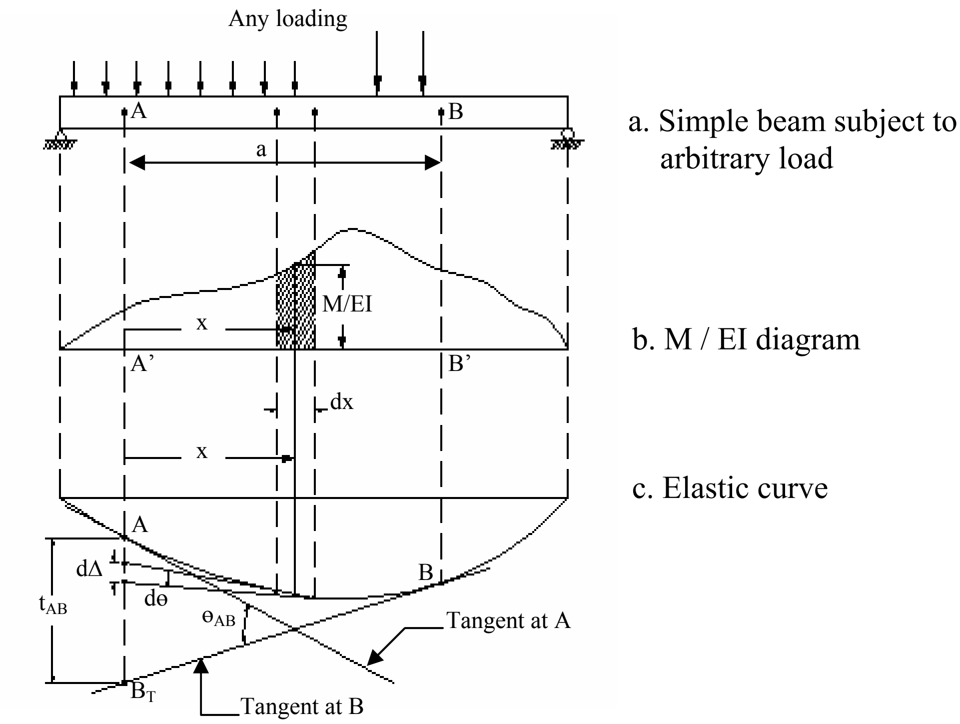

Figure 12 Analysis of deflection by moment-area method

Elastic curve equation:

$$\theta_{AB} = \int_A^B \frac{M}{EI} dx \quad \text{radian}$$

$$t_{AB} = \int_A^B \frac{Mx}{EI} dx$$

From Fig.9; $\Delta_{BA} = a\theta_{AB} - t_{BA}$

Where ; θ_{AB} = Area of M/EI between point A to point B

t_{BA} = Moment about point B of area of M/EI diagram between point A to point B

Transformed Section

The above section indicates a significant relationship: deflection varies as 1/EI. When a beam made of two materials is loaded, the different values of E for two materials lead to a different axial stiffness, AE. However, the elastic beam theory can be used if the beam is hypothetically transformed to same as material. In case of a reinforced concrete beam being customarily done by replacing the area of steel with an area of concrete by means $A_c = nA_s$, where $n = E_s/E_c$. Then consider to moment of inertia, I, a reinforced concrete beam cross section was divided into two stages shown as follows:

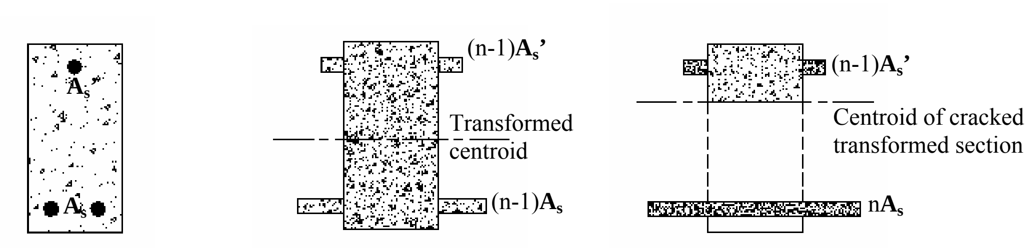

a. Beam cross section b. Uncracked transform section c. Cracked transform

Figure 13 Beam transformed section

The neutral axis of the cracked section occurs at a distance c = kd below the top of the section. For an elastic section, the neutral axis occurs at the centroid of the area, which is defined as that point where

$$\sum A_i \bar{y}_{i=0}$$

where $\bar{y}_i$ is the distance from the centroidal axis to the centroid of the i^{th} area.

MATERIALS AND METHODS

In the experiment, specimens consist of link-slab beams and monolithic beams which are of composite-beam type. To study and investigate the behaviour of simple span beams connected by link slab and a monolithic beam under flexure , the experiment was conducted as follows:

Materials

1. Concrete

Concrete used in this study has a required compressive strength of 300 kg./cm.^{2} for precast concrete beams and 200 kg./cm.^{2} for slab, keeping water-cement ratios at 0.47 and 0.65 respectively. Ordinary Portland Cement type 1 is used to mix with coarse aggregate having maximum size 3/4". Before pouring, the slump of fresh concrete was measured falling within 7.5 – 12.5 cm range. Furthermore, ∅ 15 x 30 cm. cylinder concrete specimens were cast for compressive strength test. After casting precast beams, they were cured by covering with moistened clothes for 7 days. Subsequently, link slab was cast and continuously cured until the concrete obtained adequate strength for load test.

2. Reinforcements

Two sizes of deformed bar, namely DB20 and DB25 were mainly used as a longitudinal tension reinforcement, and rounded bar, RB9 was generally used for making stirrups and as temperature steel. Initial tensile strength of deformed bar was 4,500 kg/cm.^{2} and 2,400 kg/cm.^{2} for rounded bar. Sample of each bar were randomly collected and tested for tensile strength before preparation of specimens.

3. Non–shrinkage Mortar

Non – shrinkage Mortar was used to fill the 1 cm. gap between coupled beams before proceeding casting link slab. It posses higher strength than precast beam in order to prevent crushing of the coupled beams.

Equipment

Instruments used for load test are:

1. Hydraulic jack (capacity 100 tons)

2. Load cell

3. Transfer beam

4. Strain gauge 6 mm. for concrete

5. Strain gauge 90 mm. for longitudinal bar

6. Dial gauge

7. Displacement transducer

8. Data locker

Methodology

1. General

The main objective of this study was to strengthen bridge girder by joining two adjacent simple span girders. The girders retain their dimensions and properties as before improvement. The study focused on the behavior of connection subjected to flexure. Therefore, reinforced concrete beams were used in experiment instead of precast prestressed concrete girder, which is typically used in real work, initially provided on basis of simply supported arrangement to resist positive moment at mid span. Loading frame was suitably arranged for two-point loading system. The distance between supports was set at 2.0 metres. All of test specimens were designed based on the requirements given in ACI code providing that there would be no crushing until the tension steel yielded, called tension-controlled. The specimens were divided into 2 groups of coupled beam. Each group has monolithic beam and link-slab beam to comparatively examine their behaviour with respect to flexure theory. One group was sized 20 centrimeters width and 40 centrimeters height (MB 1 and LS 1 for monolithic and link-slab beam respectively) as shown in Fig. 11, the other 30 centrimeters width and 25 centrimeters height (MB 2 and LS 2 for monolithic and link-slab beam respectively) as shown in Figure 12.

2. Specimen Preparation

All test specimens were designed as illustrated in Appendix C based on the requirements in ACI code. ACI Sec.10.3.3 attempts to prevent nonductile failures by limiting the reinforcement ratio, ρ, equal or less than 0.75 ρb. In experiment, load was applied until specimen reached the ultimate stage. Since the specimens were designed for tensile failure, crushing occurred at about middle span, reinforcement for vertical shear and horizontal shear provided exceeded the limits for tension failure.

In specimen casting, each precast beam was cast at 8 cm. shorter than designed height. Linked beam specimens were prepared by placing two precast beams of the same set (LS 1 and LS 2) end to end 1 cm. apart. Non-shrinkage mortar was used to fill the 1 cm. gap between couple beams. Reinforcement was then installed and topping concrete poured. For monolithic beams top steel reinforcement was installed and topping concrete slab poured.

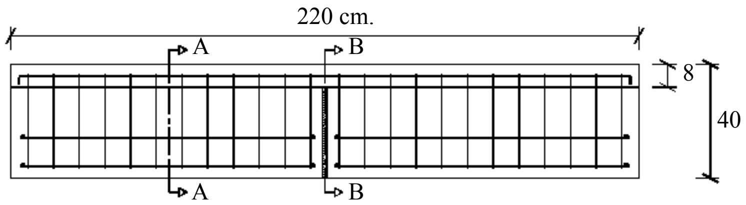

a. Lisk-slab beam, model LS1

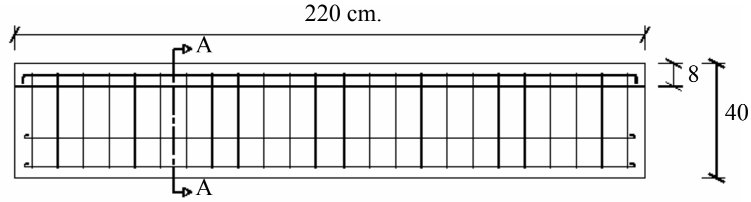

b. Monolithic beam, model MB1

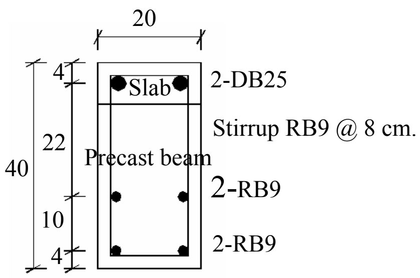

c. Section A-A

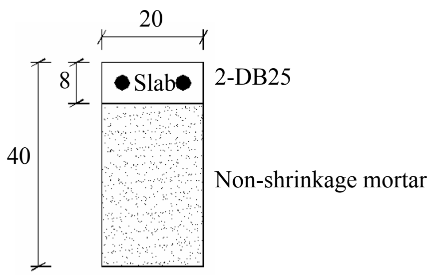

d. Section B-B

Figure 14 Link-slab beam and monolithic beam, size 20x40 cm.

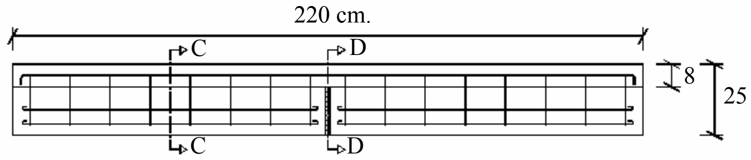

a. Link-slab beam, model LS2

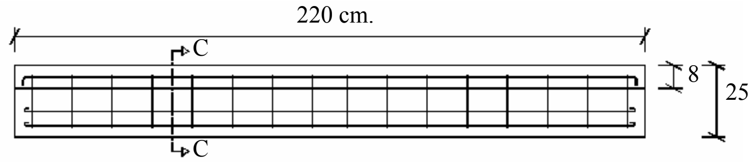

b. Monolithic beam, model MB2

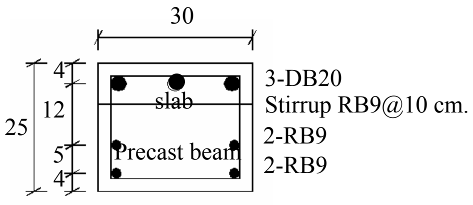

c. Section C-C

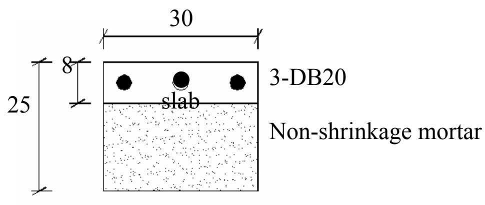

d. Section D-D

Figure 15 Link-slab beam and monolithic beam, size 30x25 cm.

3. Test Procedure

3.1 For each beam specimen, three cylindrical concrete specimens were cast and tested for compressive strength at the age of 28 days.

3.2 Two samples of each size of the steel reinforcement were tested for tensile strength.

3.3 The beam specimens were tested upside down in this study of the behavior of a link slab connection, and compared with monolithic continuity. Two types of strain gauges were used in the test, 90 mm. gauges were attached to the reinforcements, and 6 mm. gauges were attached side of the beams. The strain gauges were attached at mid span as shown in Figure 13, the point with the maximum moment. The displacement transducers were attached at the ends and middle span of the beams to measure support movement and mid-span deflection respectively. All measuring devices were directly linked to the data logger. After a specimen was placed in the simply supported arrangement, load transfer beam was placed at centre of the beam. Subsequently, load cell was installed on the transfer beam and linked with hydraulic jack as shown in Figure 13. All specimens were loaded by two point loading up to failure. Visual examination of specimens was also performed during the application of external load in order to detect the cracks appearing at the connecting joint in tension zones of connection.

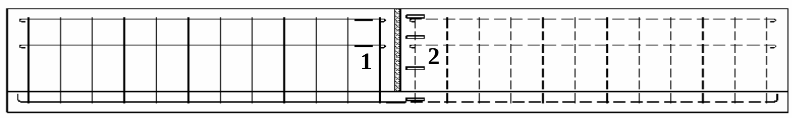

a.

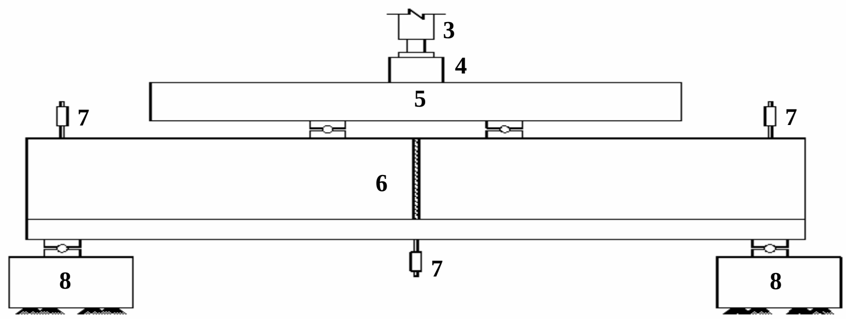

b.

1. Strain gauge at rebar
2. Strain gauge at concrete
3. Hydraulic jack
4. Load cell
5. Transfer beam
6. Test beam
7. Displacement transducer
8. Roller support

Figure 16 Experiment set up and instrumentation

RESULTS

Concrete Strength Test

The results of compressive strength tests at 28 days are shown in Table 2. It can be seen that the concrete for beams MB 1, LS 1, MB 2, LS 2 are comparable, averaging about 360 ksc., while the concrete for slab of these beam are much lower, averaging about 200 ksc.

Table 2 Compressive strength of cylindrical concrete specimen at 28 days

Specimen No.	Specimen Description	Portion	No.	Compressive Strength (ksc.)	Average (ksc.)
MB.1	Monolithic Beam Size 20 * 32 cm.	Beam	1	355.35	
			2	361.15	358.83
			3	359.99	
LS.1	Link Slab Beam Size 20 * 32 cm.	Beam	1	346.06	
			2	378.55	363.47
			3	365.79	
Topping	MB 1 & LS 1 Size 20 * 8 cm.	Slab	1	144.20	
			2	180.16	163.92
			3	167.40	
MB.2	Monolithic Beam Size 30 * 17 cm.	Beam	1	303.14	
			2	327.50	324.79
			3	343.74	
LS.2	Link Slab Beam Size 30 * 17 cm.	Beam	1	384.35	
			2	390.15	394.02
			3	407.55	
Topping	MB 2 & LS 2 Size 30 * 8 cm.	Slab	1	231.21	
			2	245.13	235.85
			3	231.21	

Reinforcement Strength Test

The results of tensile strength tests are shown in Table 3. It can be seen that the strength of deformed bar, SD 40 type, vary from about 4,400 ksc. to 5,600 ksc., while the strength of rounded bar, SR 24 type, is much higher than requirement (2,400 ksc.).

Table 3 Tensile strength of reinforcement steel

Bar Type	No.	Dia. Test (mm.)	Yield Load (kg.)	Ultimate Load (kg.)	Yield Strength (ksc.)	Aver. Yield Strength (ksc.)	Ultimate Stress (ksc.)
DB 25	1	16	8,872	12,367	4,413	4,418	6,151
	2	16	8,894	12,535	4,424		6,234
DB 20	1	16	9,864	12,115	4,906	4,916	6,026
	2	16	9,906	12,276	4,927		6,106
DB 9	1	9	2,154	2,931	3,386	3,484	4,607
	2	9	2,279	2,914	3,582		4,581

Beam Tests

The results of the beam tests which are shown in Table 4, consist of cracking and yielding loads compared with theoretical calculation. The deflections and strains during load increasing are shown in Figure 17 to Figure 18.

Table 4 Load at concrete cracking and tension steel yielding stage of specimens

Model No.	Test Results		Theoretical Calculation		Different (%)	
	Cracking (ton)	Yielding (ton)	Cracking (ton)	Yielding (ton)	Cracking	Yielding
MB.1	5.78	39.12	5.42	37.51	+ 6.6	+ 4.3
LS.1	4.12	36.63	4.02	35.85	+ 2.5	+ 2.2
MB.2	2.86	18.17	3.02	19.51	- 5.3	- 6.9
LS.2	2.58	18.96	2.86	19.45	- 9.8	- 2.5

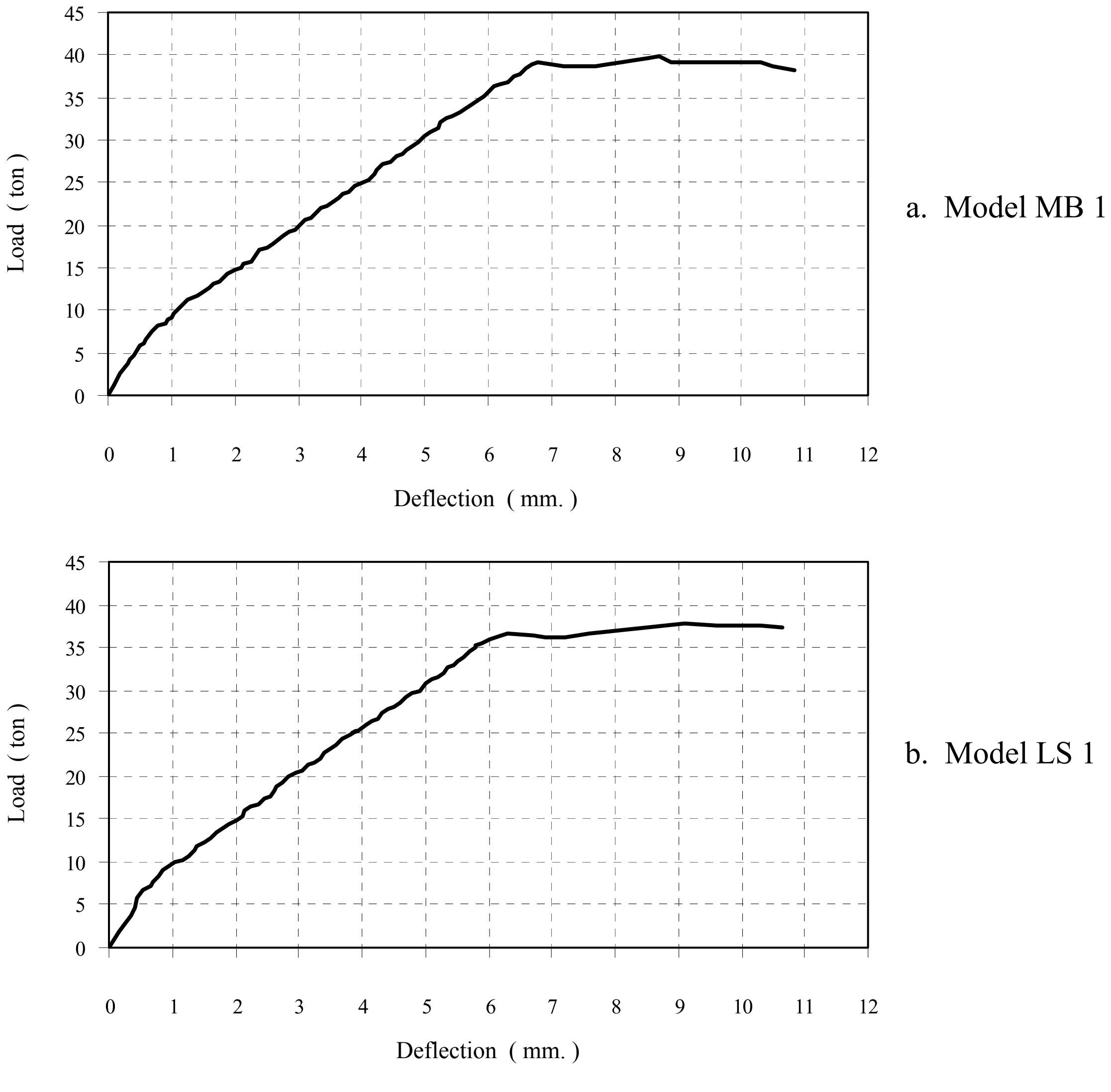

Figure 17 Load–Deflection relationship of specimens

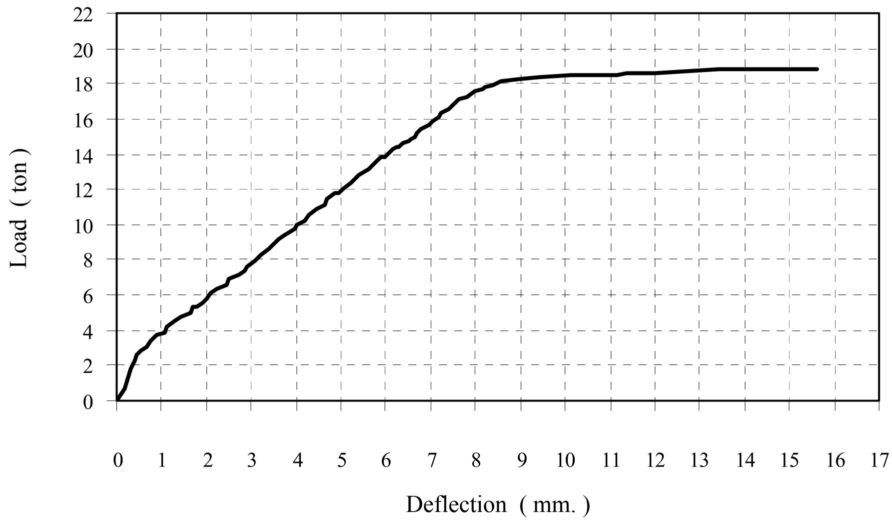

c. Model MB 2

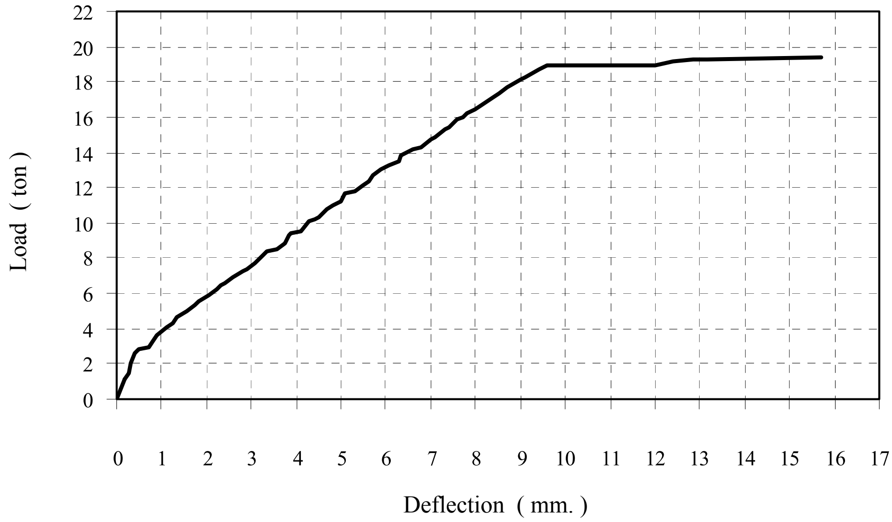

d. Model LS 2

Figure 17 (continued)

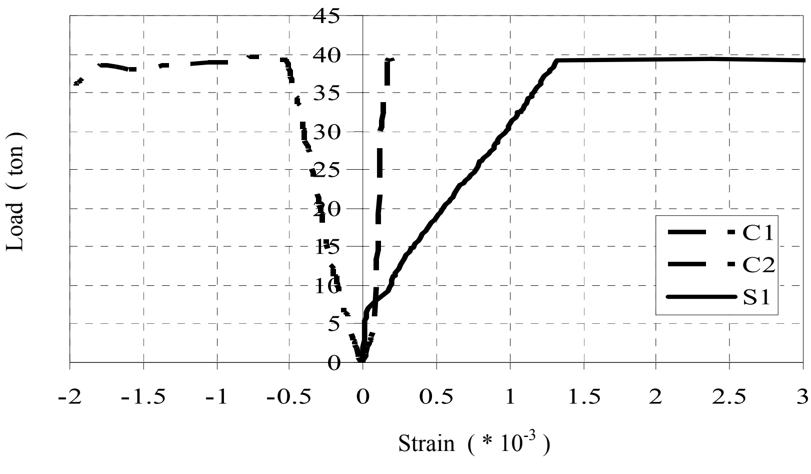

a. Model MB 1

Figure 18 Load–Strain relationship of specimens

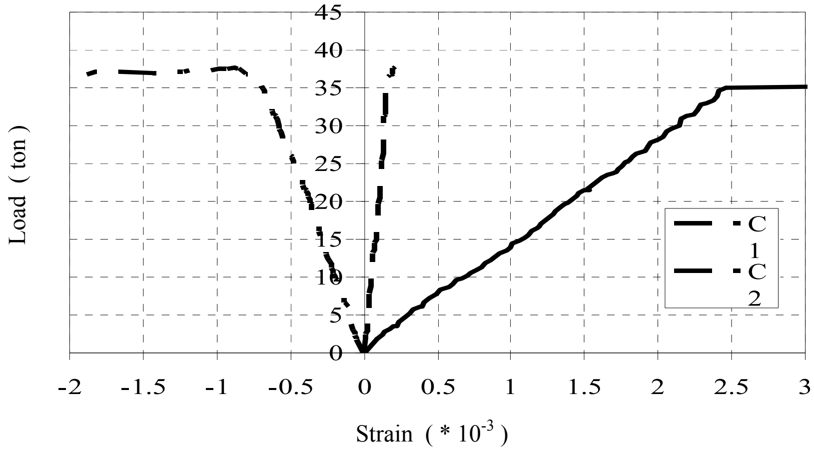

b. Model LS 1

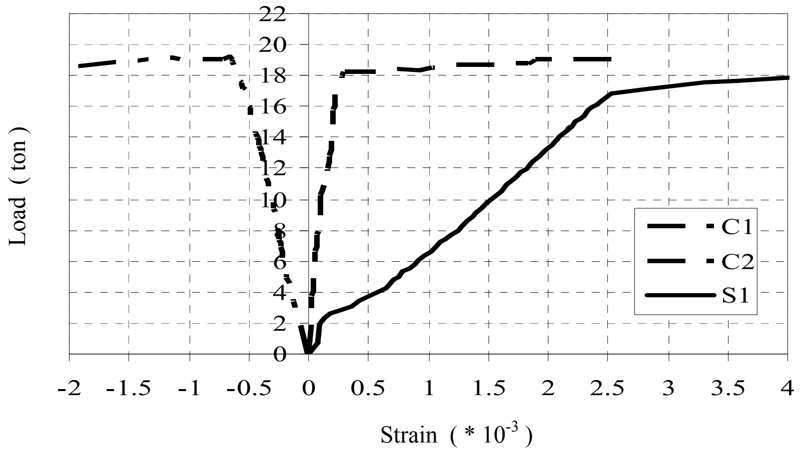

c. Model MB 2

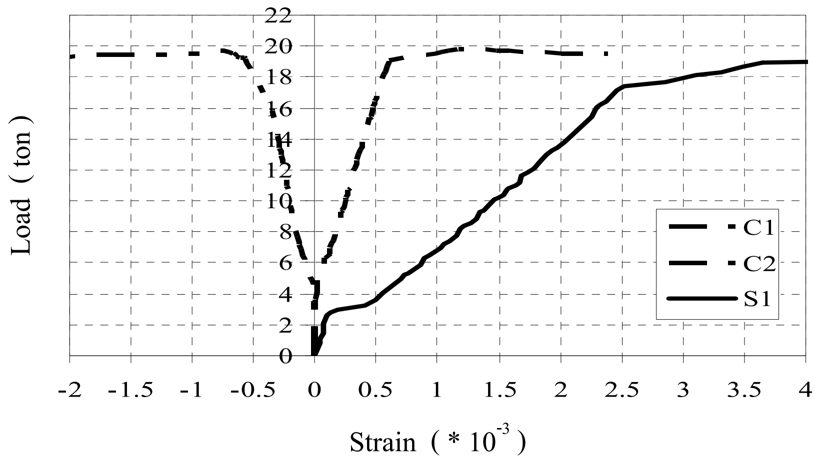

d. Model LS 2

Figure 18 (continued)

DISCUSSION

This study aimed to investigate the behavior of composite beam fabricated by connecting two precast beams by a link slab. Here, two adjacent simple-span beams were connected by link slab and tested. This method is expected to be applied in real work in the case of joining two simple-span pre-tension prestressed concrete girders. The test results of link slab compared with conventional monolithic beam were conducted to validate the principle of analysis and design of link slab. The results are discussed as follows.

1. Comparison between load resisting characteristics of link-slab and monolithic beams.

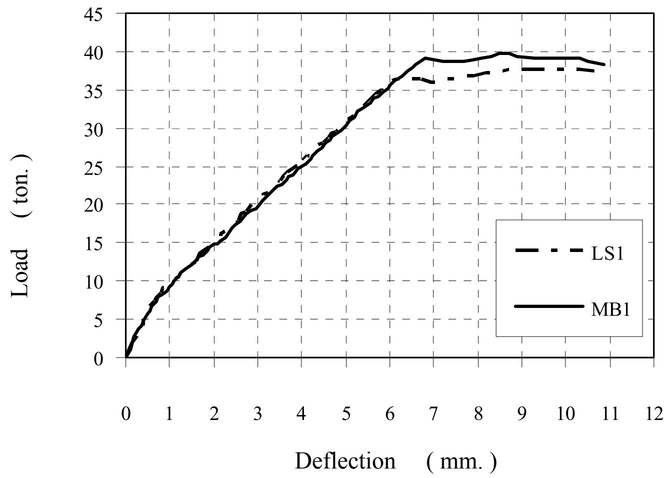

a. Model LS 1 and MB 1

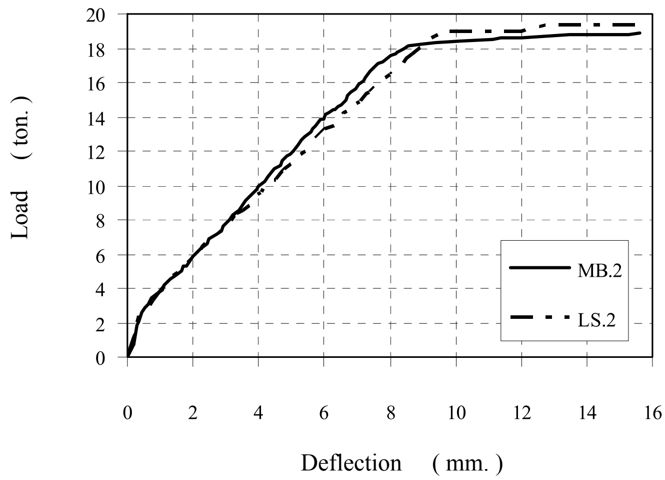

b. Model LS 2 and MB 2

Figure 19 Load–Deflection relationships of monolithic beam and link- slab beam

From Table 4 in the test results, it is apparent that the link-slab beam has ultimate load resisting capacity close to the monolithic beam of the same section. Figure 19 shows that gradient of the load-deflection curve of the link slab beam has nearly the same slope as the monolithic beam. It can be deduced that, the link-slab beam has same stiffness as the monolithic beam of the same cross section.

2. Comparison between load resisting characteristics of the specimen beams and the theory.

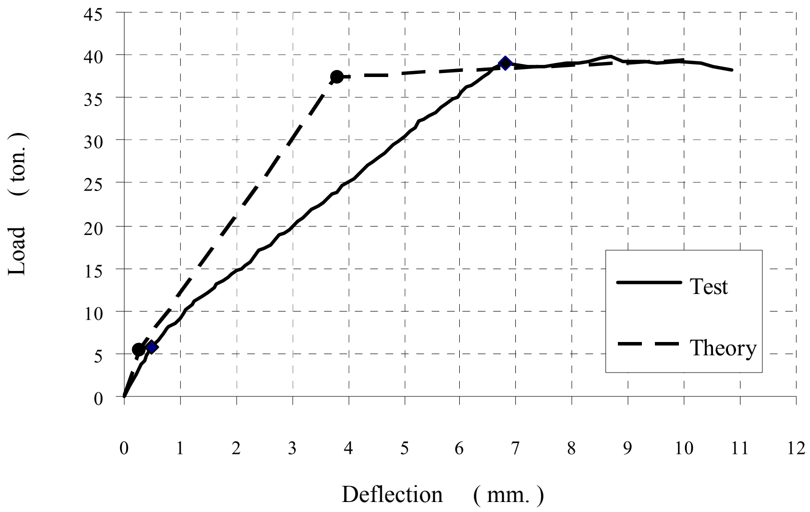

a. Model MB 1

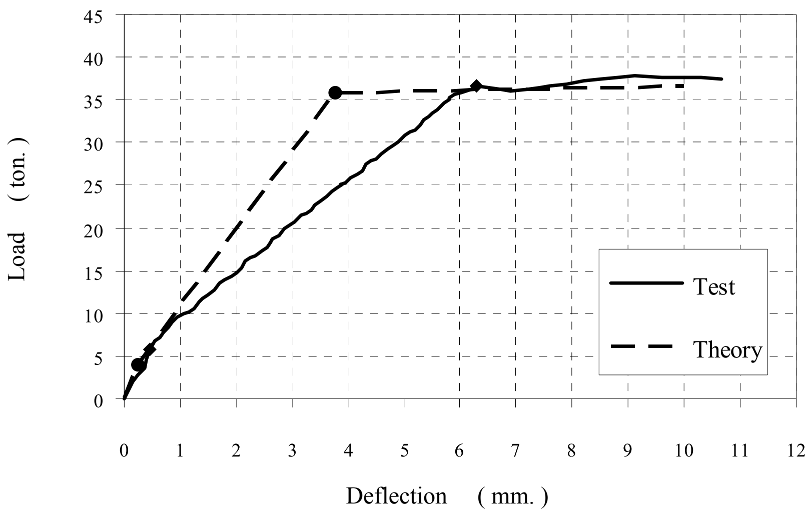

b. Model LS 1

Figure 20 Load–Deflection relationships of link slab beam and theoretical beam

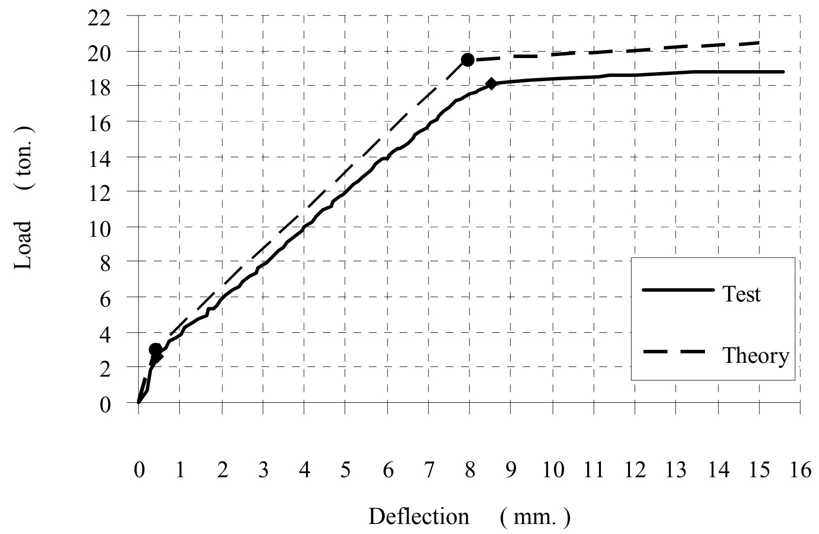

c. Model MB 2

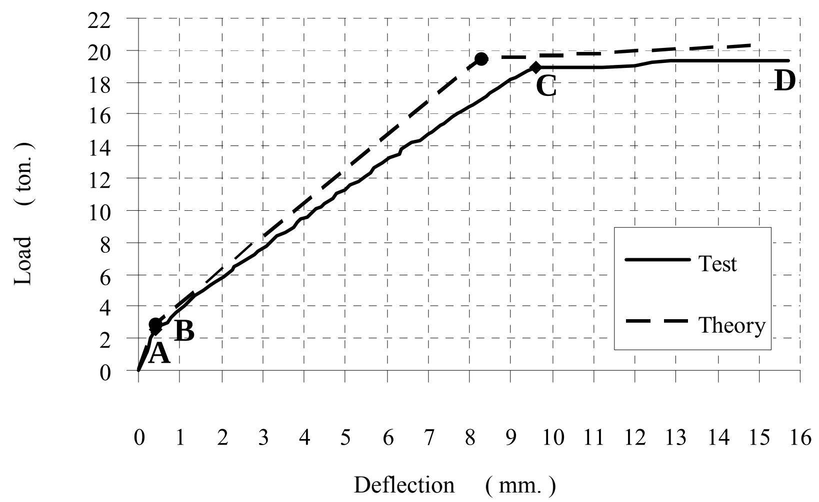

d. Model LS 2

Figure 20 (Continued)

The flexural experiment was conducted by applying two point loading on a beam. Flexure theory indicates that the deflection increases linearly with load but varies inversely with moment of inertia, I. From Fig.20, the beam was initially uncracked (section A – B), the entire cross section was stressed due to load. The moment of inertia of this section was the uncracked moment of inertia, Ig. With further load, cracking occurred when the moment reached the cracking moment, M_{cr}, at stage B. After cracking, the tensile force in the concrete was transferred to the steel. As a result, effective concrete section in resisting moment was reduced, its moment of inertia decreased leading to a decrease in stiffness of the beam. Thus the slope of the load – deflection diagram (shown by section B – C) also decreased until the reinforcement reached to the yield point at stage C. The moment of inertia after concrete cracked and right up to the yielding of steel was the cracked moment of inertia, I_{cr}. After yielding, deflection increased rapidly with very little increase in load 5(shown by section C – D). Eventually, the beam failed due to crushing of the concrete at the top of the beam.

Test results in Figure 20 shows that, both link-slab beams LS 1 and LS 2 have similar load-deflection relationship as flexural theory. However, while LS2 beam has more or less the same characteristic as in theory, LS1 beam presents some deviation in result. During experiment, LS1 beam have reacted to applied load in a less-stiff manner than in theory. This might be due to the slip of longitudinal reinforcement at connection as relatively low compressive strength was used thus causing insufficient bond strength. In addition, concrete cracking forces and tension steel yielding forces from tests and calculation are comparatively correlation. The differences between test and calculation fall within 10 percent range which seemed to be acceptable.

3. The sectional strain distribution pattern

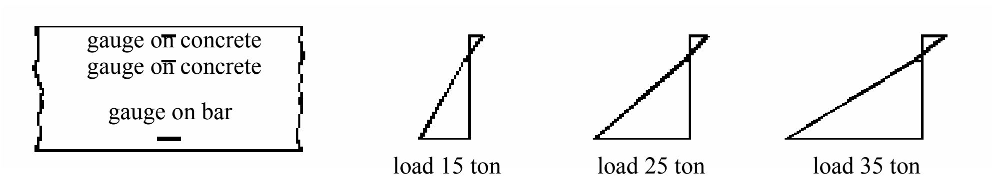

a. Monolithic beam MB 1

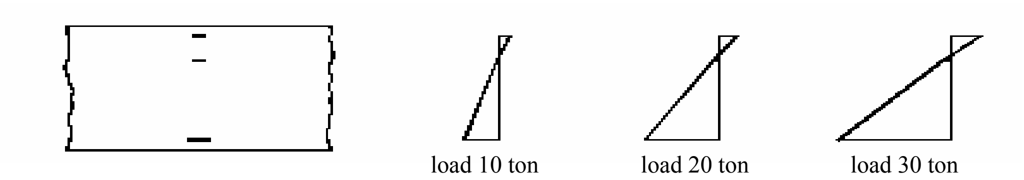

b. Link slab beam LS 1

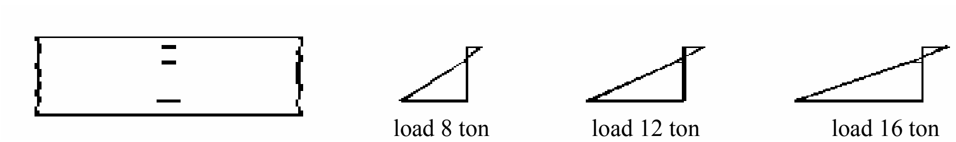

c. Monolithic beam MB 2

Figure 21 Strain distribution across section at various loading stages

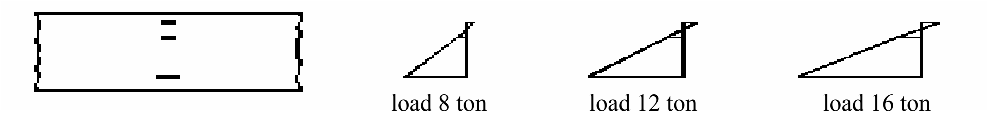

d. Link slab beam LS.2

Figure 21 (Continued)

The first basic assumption in flexure theory stated “ Sections perpendicular to the axis of bending which are plane before bending remain plane after bending ”. From the test results in Fig.21, the dots represent strains of concrete and reinforcement measured at various load increments by the strain gauges attached in all specimens. It can be seen that measured strains are approximately linear. Therefore, It can be said that all four beams obey the first assumption of flexure theory.

4. The crack pattern

(a) Specimen Model LS 1

(b) Specimen Model MB 1

Figure 22 Test specimens after failure

(c) Specimen Model LS 2

(d) Specimen Model MB 2

Figure 22 (Continued)

Although the aforementioned test indicates that the link slab beam had capacities and some behaviour like the monolithic beam, which behaved as predicted by the theory, there remains the differences in pattern of cracking. For the monolithic beam, the first crack occurred on tension fiber at mid-span of the beam. As load increased, cracks distributedly take place at other sections along the beam from mid-span to supports. The cracks expanded wider and propagated deeper into section as load increased. The direction of the fracture inclined to center of arc. For the link slab beam, initially the crack pattern in slab looked like that of the monolithic beam. As load increased, crack exceeded the depth of link slab and ran through interface between precast beam and non–shrinkage mortar at connected joint. The joint appeared separated. Consequently, rate of distributedly cracking decreased but rate of the joint separation rapidly increased until concrete crushing failure occurred with opening wider than the monolithic beam's crack.

It can be explained that, due to joint opening, moment of inertia of concrete joint reduced. The crack was concentrated only at the opening and not widely distributed throughout the beam length as in monolithic beam case. At ultimate stage it could be observed that opening of link-slab beam is wider than crack width of monolithic beam of which cracks seemed to be well distributed.

The link-slab beam LS 2 which is more shallow than beam LS 1 showed relatively well distributed cracks compared to monolithic beam in each particular group. This is because for deeper link- slab beam after crack extended beyond slab thickness, there exists relatively deeper space for opening to occur, thus causing higher rate of opening.

In constructing connectively with link slab, it should be noted that the method is suitable for plank or box girder having ratio between height to width 0.35 to 0.70 respectively. This is because girder with greater ratio than this will exhibit wide opening at load beyond concrete-crushing load and this will violate the requirement in design code at serviceability stage (crack width control).

CONCLUSION

For all four specimens designed to failure tension, the following can be concluded.

1. The behavior of the link-slab beam subjected to flexure was similar to that of the monolithic beam and correlated to flexure theory.

2. The proposed model derived from flexure theory can explain accurately the behavior of laboratory specimens.

LITERATURE CITED

American Association of State Highway and Transportation Officials, AASHTO, **"Standard Specification for Highway Bridges "** 17th Edition , 2002

Building Code Requirements for Structural Concrete. n.d. **Building Code Requirement for Structural Concrete (318 M-99X and Commentary.** (318 M-99) – ACI Committee 318.

Burke, M.P., **" The design of Integral Concrete Bridge, "** Concrete International, American Concrete Institute, V. 15, No. 6 June 1993, PP. 37 – 42

Caner, A., and Zia, P., **" Behavior and Desing of Link Slab for Jointless Bridge Decks, "** PCI Journal, May – June 1998, PP. 68 – 80

James G.MacGregor, **" Reinforced Concrete Mechanics and Design "** , Third Edition, Prentice-Hall, Inc., 1988

T.Y. Lin, and Ned H. Bums, **" Design of Prestressed concrete Structures "** , third edition, John Wiley & Sons

APPENDICES

Appendix A

Detail of Typical Plank and Box Girder

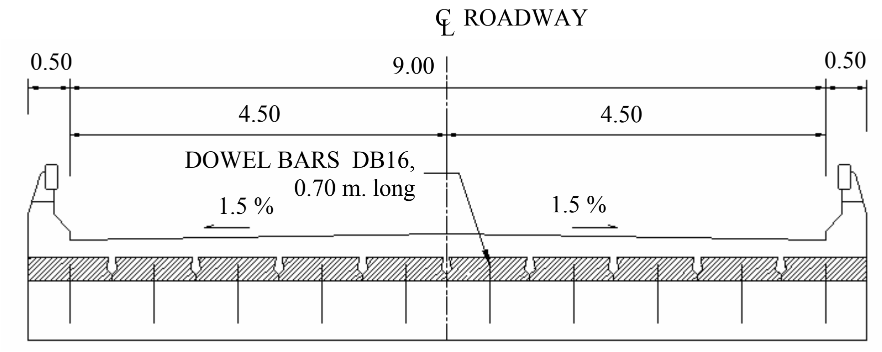

a. Cross–section of a plank girder bridge

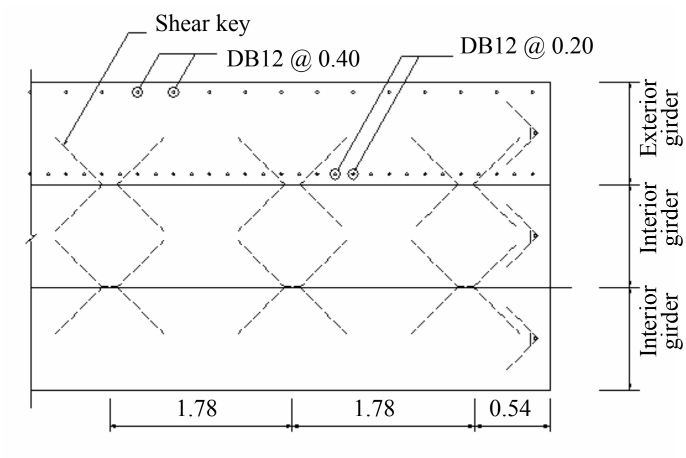

b. Arrangement of plank girder

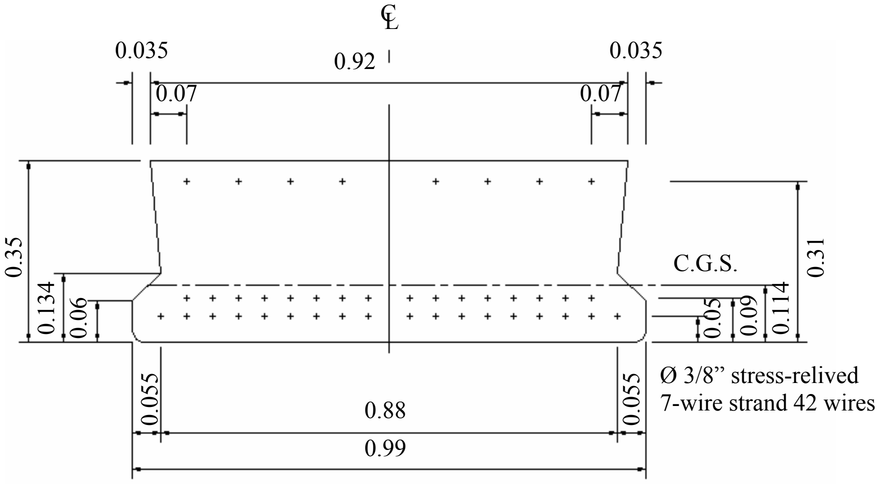

c. Arrangement of prestressing wire

Appendix Figure A1 Detail of typical plank girder

Source : The Public Works Department (1986)

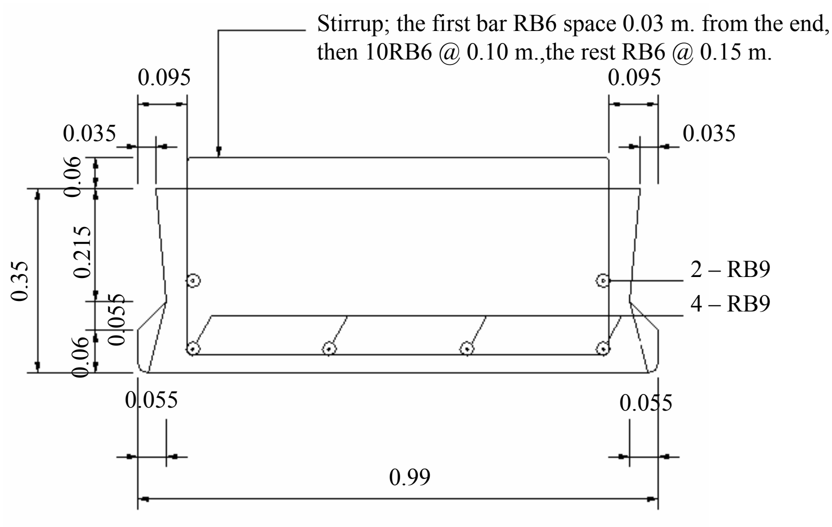

d. Arrangement of rebars

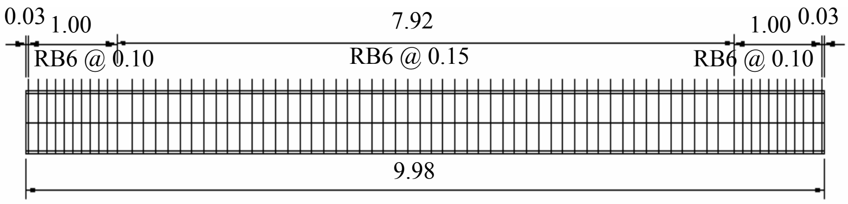

e. Profile of stirrups

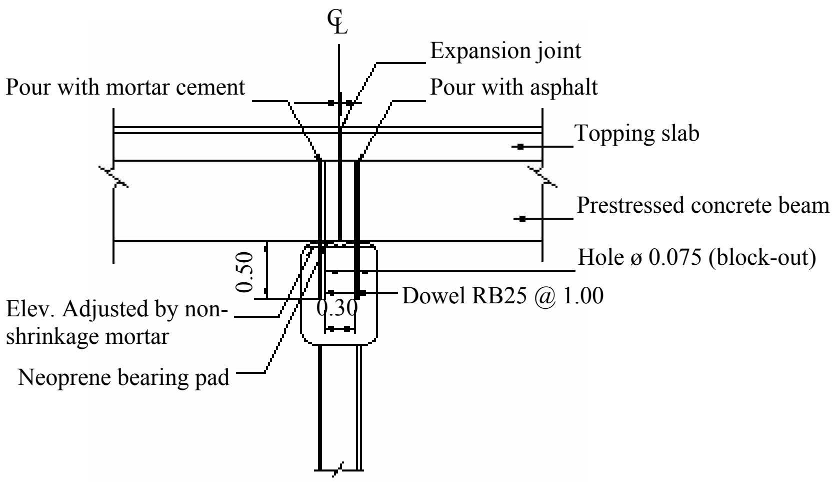

f. Typical of fixed end and free end

Appendix Figure A1 (Continued)

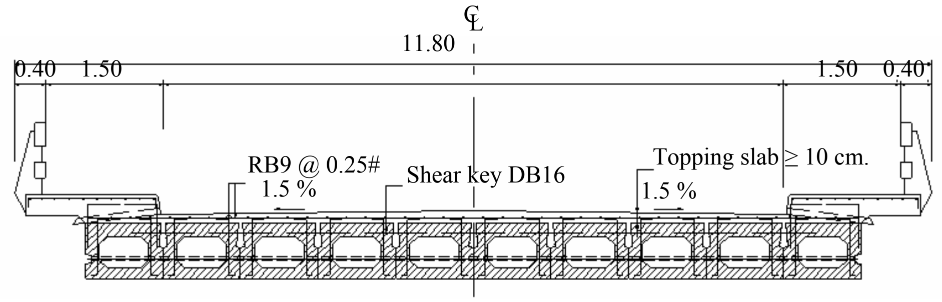

a. Cross–section 0f a box girder bridge

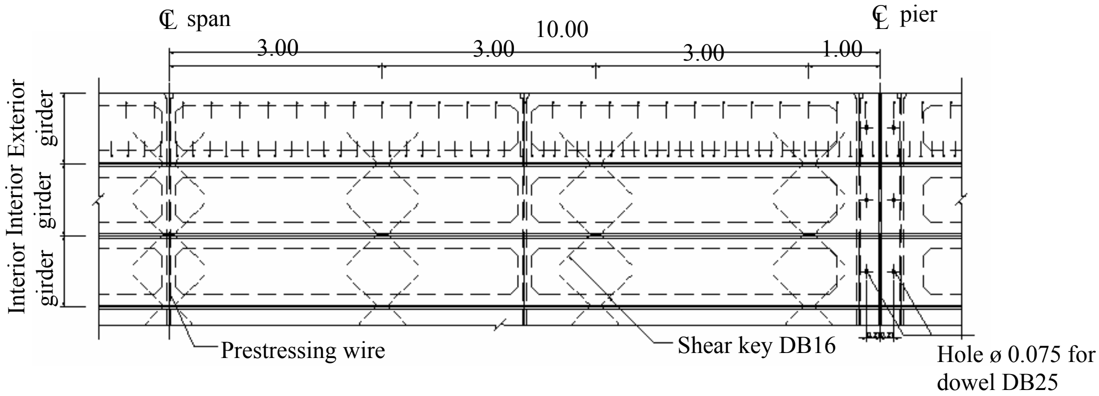

b. Arrangement of box girder

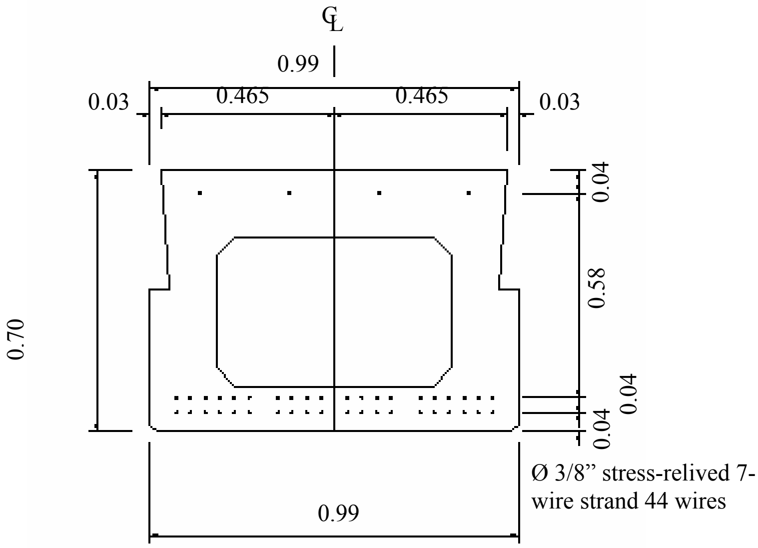

c. Arrangement of prestressing wire

Appendix Figure A2 Detail of typical box girder

Source: The Public Works Department (1986

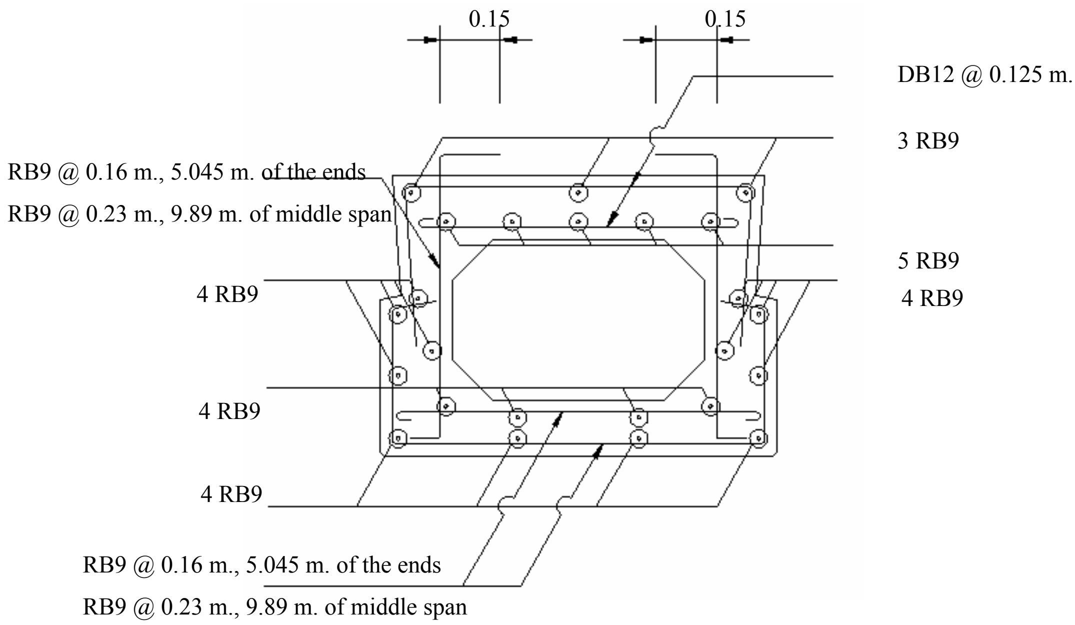

d. Arrangement of rebars

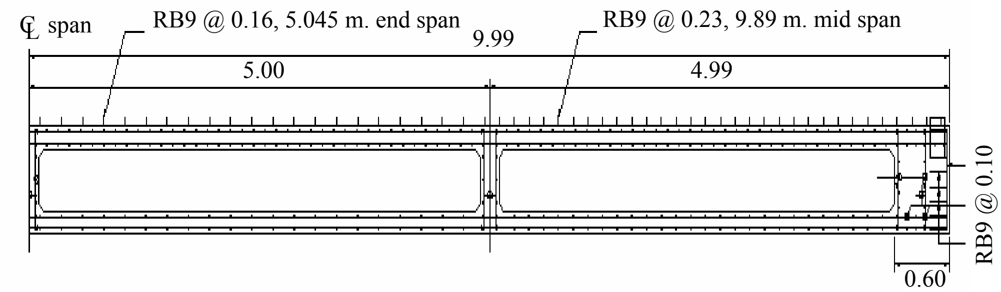

e. Profile of stirrups

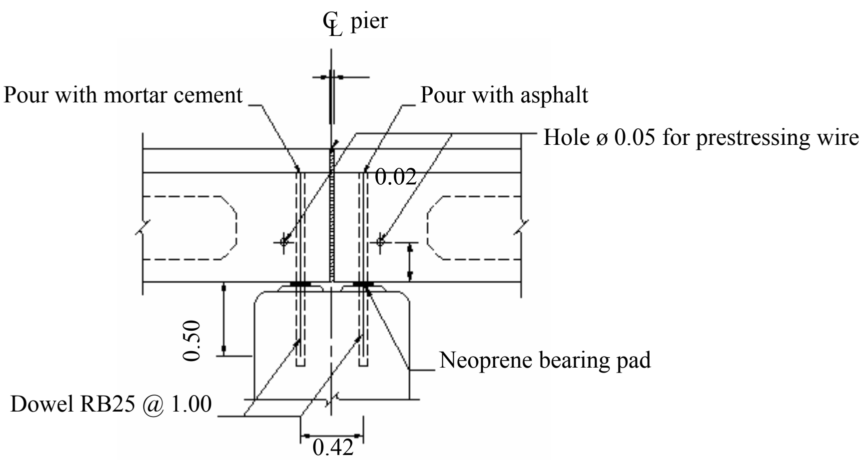

d. Typical of fixed end and free end

Appendix Figure A2 (Continued)

Appendix B

Live Load

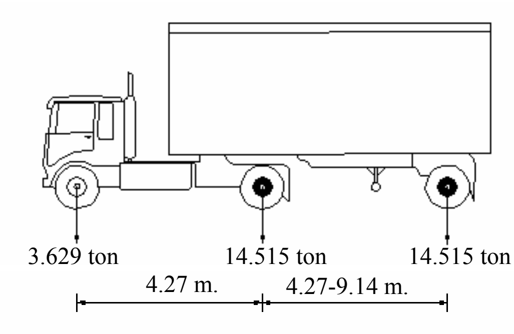

a. HS20-44 Truck

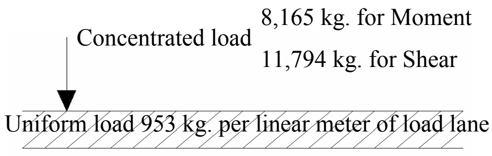

b. HS20-44 Lane

Appendix Figure B1 HS20-44 loading

Source : AASHTO (2002)

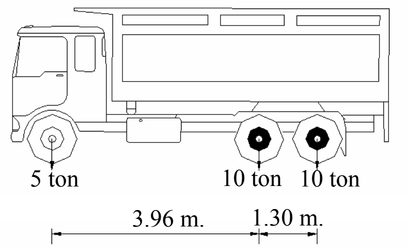

a. Truck, 3A-6W-10T

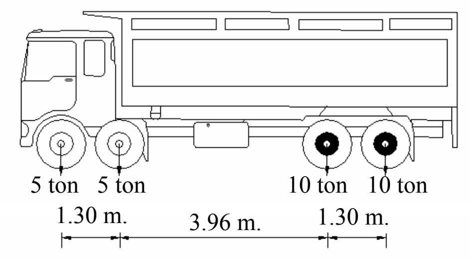

b. Truck, 4A-8W-12T

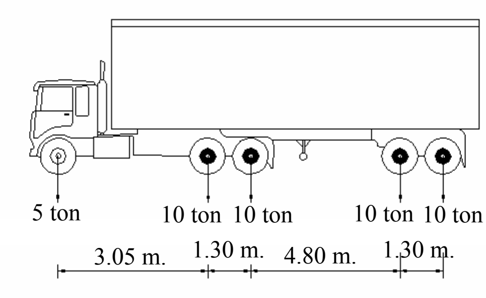

c. Semi-trailer, 2A-4W-8T

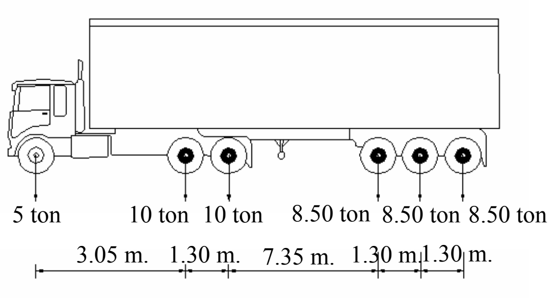

d. Semi-trailer, 3A-6W-12T

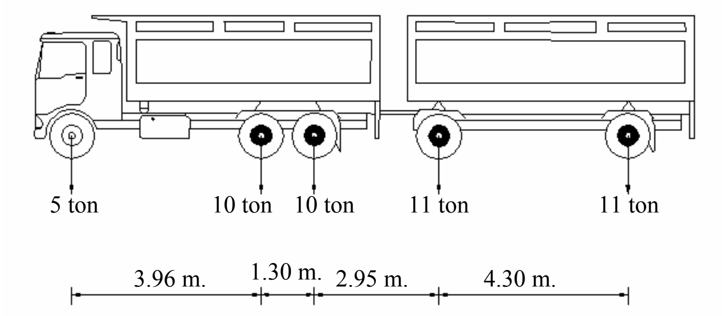

e. Trailer, 2A-4W-8T (type 1)

Appendix Figure B2 The kind of Thai trucks promulgated in 2005

Source: Department of highways (2005)

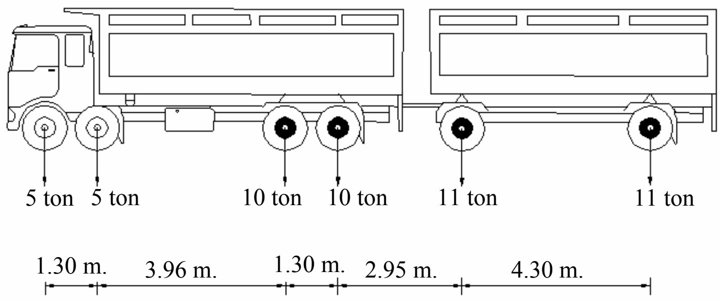

f. Trailer, 2A-4W-8T (type 2)

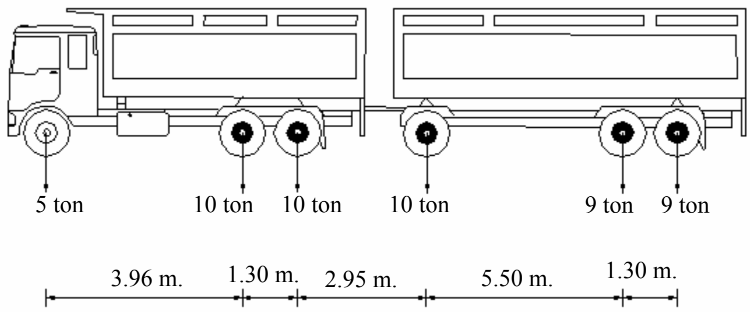

g. Trailer, 3A-6W-12T

Note : 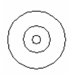 = single tire 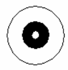 = double tire

Appendix Figure B2 (Continued)

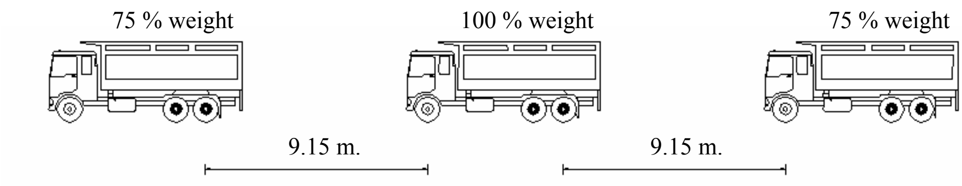

Appendix Figure B3 Arrangement of truck train

Appendix C

Design of Specimens

Design of Specimens

1. Design of Composite Beam Size 20*40 cm.

Design Conception: Strength design by elastic theory

Concrete:

Precast Beam	f_c'	=	300	ksc.
$E_c = 15{,}100\sqrt{f_c'}$		=	261,540	ksc.
Slab	f_c'	=	200	ksc.
	E_c	=	214,960	ksc.

Steel:

Reinforcing steel

rebar Ø 6 & 9 mm. ; use grade SR 24 , plain bar

f_y	=	2,400	ksc.

rebar larger than 9 mm. ; use grade SD 40 , deform bar

fy	=	4,500	ksc.
E_s	=	2.04E+06	ksc.

Composite Beam;

Precast Beam	b_b =	20	cm.	h_b =	32	cm.
Slab	b_s =	20	cm.	h_s =	8	cm.
	d =	36	cm.			

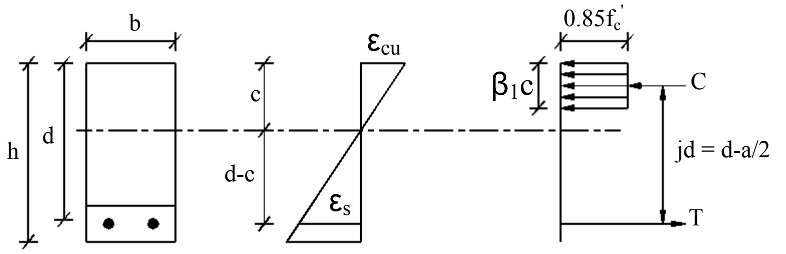

a. Cross section b. Strain distribution c. Equivalent stress block

Appendix Figure C1 Stress and strain diagram in a rectangular beam

Balance Section :

Equilibrium equation ; $C = T$

$0.85f_c'b\,a = A_sf_y$

$A_s = 0.85f_c'ba / f_y$

$A_s = \rho_b bd$; $\rho_b = 0.85f_c'a / f_y.d$

$a = \beta_1 c$; $\rho_b = 0.85f_c'\beta_1 c / f_y.d$

From strain distribution ; $c / d = \varepsilon_{cu} / (\varepsilon_{cu} + \varepsilon_y)$

$\rho_b = 0.85f_c'\beta_1.\varepsilon_{cu} / (f_y.(\varepsilon_{cu} + \varepsilon_y))$

$$\beta_1 = 0.85 - 0.05\left(\frac{f_c' - 280}{70}\right)$$

Substitute ; $\beta_1 = 0.84$

$\varepsilon_{cu} = 0.003$

$\varepsilon_y = fy / Es = 0.002$

Thus ; $\rho_b = 2.73E\text{-}02$

$A_{s,b} = 19.65$ cm.^{2}

Allowable $A_{s,max} = 0.75 A_{s,b} = 14.74$ cm.^{2}

$A_{s,min} = \sqrt{f_c'}.b_w.d / 4f_y = 0.69$ cm.^{2}

Use amount of reinforcement $= 0.50 A_{s,b} = 9.82$ cm.^{2}

Use 2 DB 25 ; $A_s = 9.82$ cm.^{2}

Check mode of failure :

Equilibrium equation ; $C = T$

$0.85f_c'b\beta_1 c = A_sf_y$

$c = 10.19$ cm.

From strain distribution ; $\varepsilon_c / c = \varepsilon_s / (d - c)$

$\varepsilon_s = \varepsilon_c*(d\text{-}c) / c$

$\varepsilon_s = 0.008 > \varepsilon_y$

Determination of Load

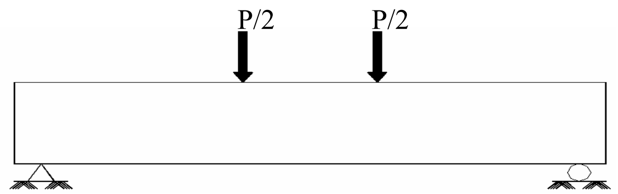

Tensile failure ; $M_{mid} = T(d - a/2) = 0.75P/2 + 95.04$

$T = A_s f_y$; Then $A_s f_y (d - a/2) = 0.75P/2 + 95.04$

where, $a = \beta_1 c$; thus $P = 18{,}575$ kg.

Determination of Stirrups

Vertical shear :

$R_L = 18{,}767$ kg.

at d ; $V_u = 18{,}708$ kg.

$V_c = 0.53\sqrt{f_c'}.b_w.d$

$= 5{,}397$ kg.

Use RB 9 as stirrup ; $A_v = 1.27$ cm.^{2}

s_{max} equal d/2 or 60 cm. Whichever is less

$d/2 = 18$ cm.

$A_{v(min)} = 0.345 b_w s / f_y$ (SI unit)

$s_{max} = 53.07$ cm.

From formula ; $s = A_v f_y d / (V_u - V_c)$

$= 8.24$ cm.

Horizontal shear :

$V_{uh} = 18{,}767$ kg.

$v_{uh} = V_{uh} / b_v.d$

$= 26.06$ ksc.

ACI Sec. 17.5.2.3 When ties are provided, and contact surface is clean, free of laitance , and intentionally roughened , shear strength shall be taken as:

$$v_{nh} = (1.8 + 0.6\rho_v f_y)\lambda \quad \text{(SI unit)}$$

Substitute; $\rho_v = 7.06E\text{-}03$

$\lambda = 1.00$

Thus ; $v_{nh} = 28.51 > v_{uh}$ **OK.**

Use stirrup RB 9 @ 0.08 m.

Minimum Reinforcing Steel in Precast Beam

$A_s \geq 0.0025bh$

≥ 1.60 cm.^{2}

Use 4-RB 9 ; $A_s = 2.54$ cm.^{2}

2. Design of Composite Beam Size 30*25 cm.

Design Conception: Strength design by elastic theory

Composite Beam;

Precast Beam	b_b =	30	cm.	h_b =	17	cm.
Slab	b_s =	30	cm.	h_s =	8	cm.
	d =	21	cm.			

Similar to design of composite beam Size 20*40 cm.

$$\rho_b = 0.85f_c'\beta_1.\varepsilon_{cu} / f_y.(\varepsilon_{cu} + \varepsilon_y)$$

Thus ; ρ_b = 2.73E-02

$A_{s,b}$ = 17.19 $cm.^2$

Allowable $A_{s,max} = 0.75\ A_{s,b}$ = 12.89 $cm.^2$

$A_{s,min} = \sqrt{f_c'}.b_w.d / 4f_y$ = 0.61 $cm.^2$

Use amount of reinforcement = 0.50 $A_{s,b}$ = 8.60 $cm.^2$

Use 3 DB 20 ; A_s = 8.52 $cm.^2$

Check mode of failure :

Equilibrium equation ; C = T

$0.85f_c'b\beta_1c = A_sf_y$

c = 6.00 cm.

From strain distribution ; $\varepsilon_c / c = \varepsilon_s / (d - c)$

$\varepsilon_s = \varepsilon_c*(d-c) / c$

ε_s = 0.00751 > ε_y

Thus, the section as being tension - controlled.

Determination of Load

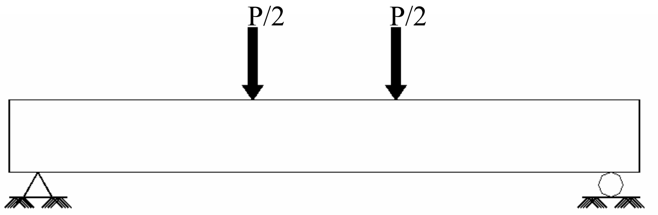

Tensile failure ;	$M_n = T (d - a / 2)/100$	=	$0.75P/2 + 89.10$	
$T = A_s f_y$; Then	$A_s f_y (d - a / 2)/100$	=	$0.75P/2 + 89.10$	
	P	=	9,335	kg.

Determination of Stirrups

Vertical shear :

	R_L	=	9,533	kg.
at d ;	V_u	=	9,477	kg.
	V_c	=	$0.53\sqrt{f_c'}.b_w.d$	
		=	4,722	kg.
Use RB 9 as stirrup ; A_v		=	1.27	$cm.^2$

s_{max} equal d/2 or 60 cm. Whichever is less

	$d / 2$	=	11	cm.
	$A_{v\,(min)}$	=	$0.345 b_w s/f_y$	(SI unit)
	s_{max}	=	35.38	cm.
From formula ;	s	=	$A_v f_y d / (V_u - V_c)$	
		=	13.46	cm.

Horizontal shear :

	V_{uh}	=	9,533	kg.
	v_{uh}	=	$V_{uh} / b_v.d$	

$= 15.13$ ksc.

ACI Sec. 17.5.2.3 When ties are provided , and contact surface is clean , free of laitance , and intentionally roughened , shear strength shall be taken as

$v_{nh} = (1.8 + 0.6\rho_v f_y)\lambda$ (SI unit)

Substitute; $\rho_v = 7.06E\text{-}03$

$\lambda = 1.00$

Thus ; $v_{nh} = 28.51$ $> v_{uh}$ **OK.**

Use stirrup RB 9 @ 0.10 m.

Minimum Reinforcing Steel in Precast Beam

$A_s \geq 0.0025bh$

≥ 1.28 $cm.^2$

Use 4-RB 9 ; $A_s = 2.54$ $cm.^2$

Appendix D

Calculation of Load and Deflection

Determination of Load and Deflection at Point of Cracking and Yielding

Specimen Model MB 1

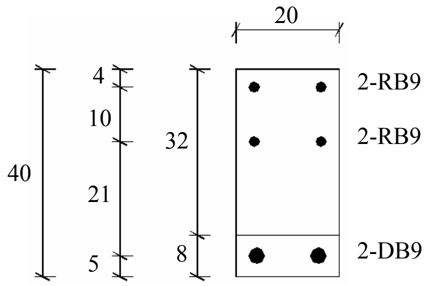

$f_{c}'_{\,(beam)}$	=	358.83	ksc.
$f_{c}'_{\,(slab)}$	=	163.92	ksc.
$f_{y\,(DB\,25)}$	=	4,418	ksc.
$f_{y\,(RB\,9)}$	=	3,484	ksc.

Appendix Figure D1 Composite beam cross-section Model MB 1

Section Properties:

$E_{c\,(beam)}$	=	286,036	ksc.	$E_{c\,(slab)}$	=	193,327 ksc.
E_s	=	2.04E+06	ksc.			
$b_{E\,(slab)}$	=	$b_{(s)} \cdot E_{(s)} / E_{(b)}$	=	13.52	cm.	
n	=	E_s / E_c	=	7.13		

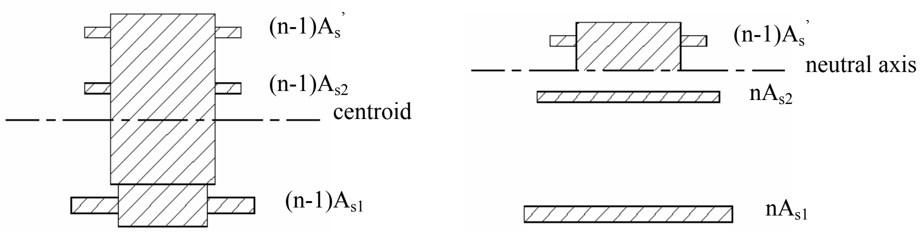

a. Uncracked transformed b. Cracked transformed section

Appendix Figure D2 Transformed section Model MB 1

Uncracked Transformed Section

The centroid of the transformed section is located at :

Element	Area	y	Ay
Beam	640.00	24.00	15,360
Slab	108.14	4.00	433
$Bar_{(\text{ upper })}$	7.80	36.00	281
$Bar_{(\text{ interm })}$	7.80	26.00	203
$Bar_{(\text{ lower })}$	60.22	5.00	301
$\sum$	823.96		16,577
ỹ	=	20.12	cm. from bottom

The moment of inertia of uncracked section:

Element	Area	y	I_g	Ay^2
Beam	640.00	3.88	54,613	9,639
Slab	108.14	- 16.12	577	28,098
$Bar_{(\text{ upper })}$	7.80	15.88	-	1,967
$Bar_{(\text{ interm })}$	7.80	5.88	-	270
$Bar_{(\text{ lower })}$	60.22	- 15.12	-	13,764
$\sum$			55,190	53,739
	I_{gt}	=	108,929	$cm.^4$

Cracked Transformed Section

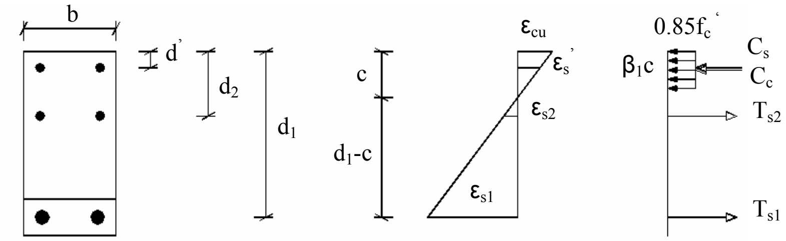

a. Beam cross-section b. Strain distribution c. Rectangular stress block

Appendix Figure D3 Strain and stress in the rectangular beam Model MB 1

If the lower steel yielded :

From equilibrium ; $C_c + C_s = T_{s1}+T_{s2}$

$$0.85f_c^{'}b\beta_1 c + A_s^{'}f_s^{'} = A_{s1}f_{y1}+A_{s2}f_{s2}$$

Determine $f_s^{'}$:

$$f_s^{'} = \varepsilon_s^{'}E_s$$

From strain distribution Appendix Figure D 3 (b.)

$$\varepsilon_s^{'} / (c-d^{'}) = \varepsilon_{cu} / c$$

$$\varepsilon_s^{'} = \varepsilon_{cu}(1-d^{'}/c)$$

Determine f_{s2} :

$$f_{s2} = \varepsilon_{s2}E_s$$

From strain distribution Appendix Figure D 3 (b)

$$(\varepsilon_{s2}+\varepsilon_{cu}) / d_2 = \varepsilon_{cu} / c$$

$$\varepsilon_{s2} = \varepsilon_{cu}(d_2/c-1)$$

Substitute: $(0.85f_c^{'}b\beta_1 c)+[A_s^{'}E_s\varepsilon_{cu}(1-d^{'}/c)] = A_{s1}f_{y1}+A_{s2}E_s\varepsilon_{cu}(d_2/c -1)$

$$(0.85f_c^{'}b\beta_1)c^2 + [(A_s^{'}E_s\varepsilon_{cu})-(A_{s1}f_{y1})+(A_{s2}E_s\varepsilon_{cu})]c-[(A_s^{'}E_s\varepsilon_{cu}d^{'})+(A_{s2}E_s\varepsilon_{cu}d_2)] = 0$$

Where $\beta_1 = 0.85-0.05(f_c^{'}-280)/70$

$$= 0.79$$

Thus, the neutral axis $c = 9.00$ cm.

Check whether $f_{s1} = f_{y1}$ i.e., the lower steel yield :

$$(\varepsilon_{s1} + \varepsilon_{cu})/d_1 = \varepsilon_{cu}/c$$

$$\varepsilon_{s1} = \varepsilon_c(d_1/c-1)$$

If $\varepsilon_{s1} \geq \varepsilon_{y1}$, then $f_{s1} = f_{y1}$

$$\varepsilon_{y1} = f_{y1}/E_s$$

$$= 0.002$$

$$\varepsilon_{s1} = 0.009 \quad > \varepsilon_{y1}$$

Thus, the section as being tension - controlled.

Therefore, from Appendix Figure D 2(b) and c able to obtain the moment of inertia of cracked section, I_{cr} :

Element	Area	y	I_g	Ay^2
Beam	180.00	4.50	1,215	3,645
$Bar_{(upper)}$	7.80	5.00	-	195
$Bar_{(interm)}$	9.07	- 5.00	-	227
$Bar_{(lower)}$	70.04	- 26.00	-	47,344
$\sum$			1,215	51,411
I_{cr}		=	52,626	cm.^{4}

1. Determine the Flexural Cracking Moment, M_{cr}

$$M_{cr} = f_r . I_g / y_t$$

$$f_r = 1.98\sqrt{f_c^{'}}$$

$$= 37.51 \text{ ksc.}$$

Thus ; $M_{cr} = 2{,}031$ kg.-m.

2. Determine the Nominal Moment Strength, M_n

M_n = T_r*lever arm

T_{s1} = 43,385 kg.

T_{s2} = 4,325 kg.

T_{result} = 47,710 kg.-m.

Calculate centroid of the resultant compression :

C_c = 43,575 kg.

C_s = 4,325 kg.

Centroid of compression = 3.61 cm. from top

Centroid of tension = 6.90 cm. from bottom

Thus ; M_n = 14,068 kg.-m.

3. Determine Load and Deflections due to M_{cr} & M_n

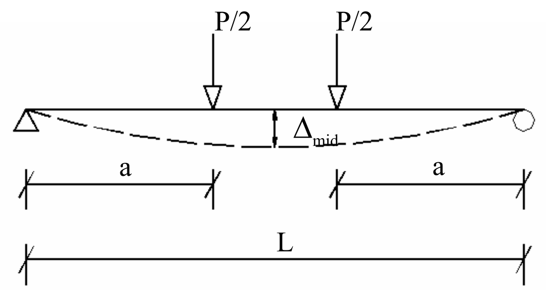

Appendix Figure D4 Deflection of simple beam under two point loading

M_{mid} = 0.5Pa

Δ_{mid} = $(P/2)L^3/ 6EI *(3a/4L - (a/L)^3)$

Therefore, load and deflection at cracking and yielding of Model MB 1

Point	Moment (kg.-m.)	P (kg.)	I ($cm.^4$)	Δ_{mid} (mm.)
Cracking	2,031	5,415	108,929	0.26
Yielding	14,068	37,514	52,626	3.80

Specimen Model LS 1

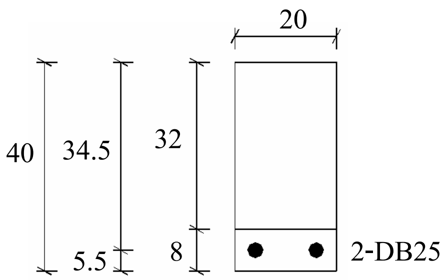

f_c' (beam)	=	363.47	ksc.
f_c' (slab)	=	163.92	ksc.
f_y (DB 25)	=	4,418	ksc.

Appendix Figure D5 Composite beam cross-section Model LS 1

Section Properties

E_c (beam)	=	287,880	ksc.	E_c (slab)	=	193,327 ksc.
E_s	=	2.04E+06	ksc.			
b_E (slab)	=	$b_{(s)} \cdot E_{(s)} / E_{(b)}$	=	13.43	cm.	
n	=	E_s / E_c	=	7.09		

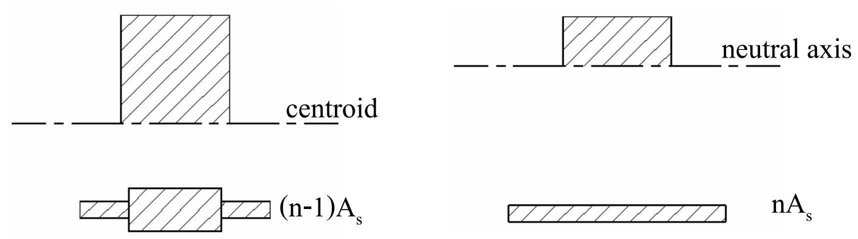

a. Uncracked transformed　　b. Cracked transformed section

Appendix Figure D6 Transformed section Model LS 1

Uncracked Transformed Section:

An elastic section, the neutral axis occurs at the centroid of the area, which is defined as that point where $\sum A_i \bar{y}_i = 0$

Element	Area	y	Ay
Beam	20c	c/2	$10c^2$
Slab	107.45	c-36	107.45c-3868.20
Bar	59.77	c-34.5	59.77c-2062.07
$\sum$			$10c^2$+167.22c-5930.27
	c	=	17.39 cm.

The moment of inertia of uncracked section :

Element	Area	y	I_g	Ay^2
Beam	347.80	8.70	8,765	26,295
Slab	107.45	- 18.61	573	37,213
Bar	59.77	- 17.11	-	17,497
$\sum$			9,338	81,005
	I_{gt}	=	90,343	$cm.^4$

Cracked Transformed Section

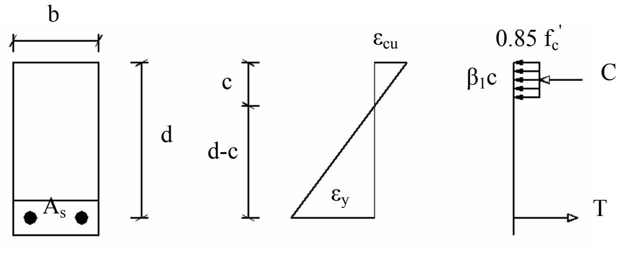

a. Beam cross-section b. Strain distribution c. Rectangular stress block

Appendix Figure D7 Strain and stress in the rectangular beam Model LS 1

If the lower steel yielded :

From equilibrium ; $C = T$

$$0.85f_c^{'}b\beta_1 c \quad = \quad A_s f_y$$

$$c \quad = \quad A_s f_y/(0.85f_c^{'}b\beta_1)$$

Substitute ; $\beta_1 \quad = \quad 0.85\text{-}0.05(f_c^{'}\text{-}280)/70$

$$= \quad 0.79$$

Thus, neutral axis $c \quad = \quad 8.88$ cm.

Check whether $f_s = f_y$ i.e., the lower steel yield :

$$(\varepsilon_s + \varepsilon_{cu})/d \quad = \quad \varepsilon_{cu}/c$$

$$\varepsilon_s \quad = \quad \varepsilon_{cu}(d/c\text{-}1)$$

If $\varepsilon_s \geq \varepsilon_y$, then $f_s = f_y$

$$\varepsilon_y \quad = \quad f_y/E_s \quad = \quad 0.002$$

$$\varepsilon_s \quad = \quad 0.009 \quad > \quad \varepsilon_y$$

Thus, the section as being tension - controlled.

Therefore, from Appendix Figure D 6(b) and c able to obtain the moment of inertia of cracked section, I_{cr} :

Element	Area	y	I_g	Ay^2
Beam	177.67	4.44	1,168	3,505
Bar	69.59	- 25.62	-	45,663
$\sum$			1,168	49,169
I_{cr}		=	50,337	cm.^{4}

1. Determine the Flexural Cracking moment, M_{cr}

$$M_{cr} = f_r . I_g / y_t$$

$$f_r = 1.98\sqrt{f_c^{'}}$$

$$= \quad 37.75 \text{ ksc.}$$

Thus ; $M_{cr} \quad = \quad 1,508$ kg.-m.

2. Determine the Nominal Moment Strength, M_n

$$M_n \quad = \quad T^*(d\text{-}a/2)$$

$= A_s f_y(d-a/2)$

Thus ; $M_n = 13{,}445$ kg.-m.

3. Determine Load and Deflections due to M_{cr} & M_n

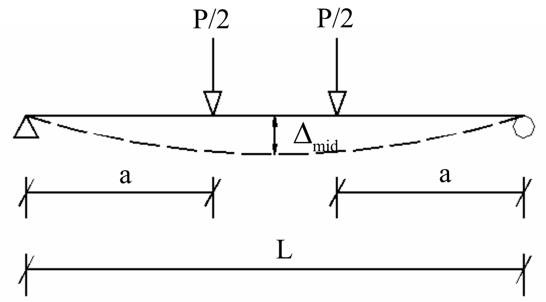

Appendix Figure D8 Deflection of simple beam under two point loading

$$M_{mid} = 0.5Pa$$

$$\Delta_{mid} = (P/2)L^3/6EI^*(3a/4L-(a/L)^3)$$

Therefore, load and deflection at cracking and yielding of Model LS 1

Point	Moment (kg.-m.)	P (kg.)	I ($cm.^4$)	Δ_{mid} (mm.)
Cracking	1,508	4,022	90,343	0.24
Yielding	13,445	35,853	50,337	3.77

Specimen Model MB 2

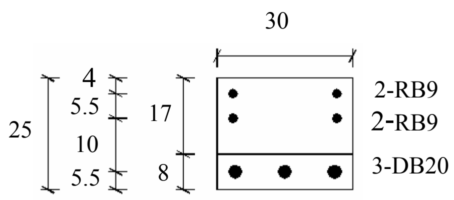

f_c' (beam) = 324.80 ksc.

f_c' (slab) = 235.85 ksc.

$f_{y\,(DB\,20)}$ = 4,916 ksc.

$f_{y\,(RB\,9)}$ = 3,484 ksc.

Appendix Figure D9 Composite beam cross-section Model MB 2

Section Properties:

$E_{c\,(beam)}$ = 272,135 ksc. $E_{c\,(slab)}$ = 231,897 ksc.

E_s = 2.04E+06 ksc.

$b_{E\,(slab)}$ = $b_{(s)} \cdot E_{(s)} / E_{(b)}$ = 25.56 cm.

n = E_s / E_c = 7.50

Uncracked Transformed Section

Similar to Model MB 1, the centroid of the transformed section is located at :

Element	Area	y	Ay
Beam	510.00	16.50	8,415
Slab	204.51	4.00	818
$Bar_{(upper)}$	8.26	21.00	174
$Bar_{(interm)}$	8.26	15.50	128
$Bar_{(lower)}$	55.35	5.50	304
$\sum$	786.39		9,839

$\tilde{y}$ = 12.51

The moment of inertia of uncracked section :

Element	Area	y	I_g	Ay^2
Beam	510.00	3.99	12,283	8,112
Slab	204.51	- 8.51	1,091	14,817
$Bar_{(upper)}$	8.26	8.49	-	595
$Bar_{(interm)}$	8.26	2.99	-	74
$Bar_{(lower)}$	55.35	- 7.01	-	2,721
$\sum$			13,373	26,319
I_{gt}		=	39,693	cm.^{4}

Cracked Transformed Section:

Similar to Model MB 1

$$(0.85f_c^{'}b\beta_1)c^2+[(A_s^{'}E_s\varepsilon_{cu})-(A_{s1}f_{y1})+(A_{s2}E_s\varepsilon_{cu})]c-[(A_s^{'}E_s\varepsilon_{cu}d^{'})+(A_{s2}E_s\varepsilon_{cu}d_2)] = 0$$

Substitute ; $\beta_1 = 0.85-0.05(f_c^{'}-280)/70$

$= 0.82$

Thus, the neutral axis $c = 6.32$ cm.

Check whether $f_{s1} = f_{y1}$ i.e., the lower steel yield :

$$(\varepsilon_{s1}+\varepsilon_c)/d_1 = \varepsilon_c/c$$

$$\varepsilon_{s1} = \varepsilon_c(d_1/c-1)$$

If $\varepsilon_{s1} \geq \varepsilon_{y1}$, then $f_{s1} = f_{y1}$

$$\varepsilon_{y1} = f_{y1}/E_s$$

$$= 0.002$$

$$\varepsilon_{s1} = 0.006 \quad > \varepsilon_{y1}$$

Thus, the section as being tension - controlled.

Therefore, from Appendix Figure D 2(b) and c able to obtain the moment of inertia of cracked section, I_{cr} :

Element	Area	y	I_g	Ay^2
Beam	189.60	3.16	631	1,893
$Bar_{(upper)}$	8.26	2.32	-	44
$Bar_{(interm)}$	9.54	- 3.18	-	96
$Bar_{(lower)}$	63.87	- 13.18	-	11,095
$\sum$			631	13,129
I_{cr}		=	13,760	$cm.^4$

1. Determine the Flexural Cracking Moment, M_{cr}

$$M_{cr} = f_r . I_g / y_t$$

$$f_r = 1.98\sqrt{f_c^{'}}$$

= 35.68 ksc.

Thus ; M_{cr} = 1,132 kg.-m.

2. Determine the Nominal Moment Strength, M_n

M_n = T_r*lever arm

T_{s1} = 41,888 kg.

T_{s2} = 3,917 kg.

T_{result} = 45,805 kg.-m.

Calculate centroid of the resultant compression :

C_c = 42,818 kg.

C_s = 2,858 kg.

Centroid of compression = 2.67 cm. from top

Centroid of tension = 6.36 cm. from bottom

Thus ; M_n = 7,316 kg.-m.

3. Determine Load and Deflections due to M_{cr} & M_n

Similar to Model MB 1

$$M_{mid} = 0.5Pa$$

$$\Delta_{mid} = (P/2)L^3/ 6EI *(3a/4L-(a/L)^3)$$

Therefore, load and deflection at cracking and yielding of Model MB 2

Point	Moment (kg.-m.)	P (kg.)	I ($cm.^4$)	Δ_{mid} (mm.)
Cracking	1,132	3,019	39,693	0.43
Yielding	7,316	19,508	13,760	7.94

Specimen Model LS 2

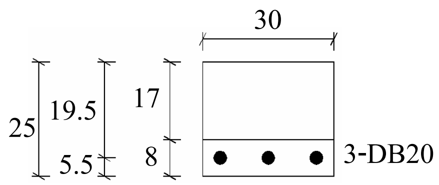

f_c' (beam) = 394.02 ksc.

f_c' (slab) = 235.85 ksc.

f_y (DB 20) = 4,916 ksc.

Appendix Figure D10 Composite beam cross-section Model LS 2

Section Properties

$E_{c\ (beam)}$	=	299,734	ksc.	$E_{c\ (slab)}$	=	231,897 ksc.
E_s	=	2.04E+06	ksc.			
$b_{E\ (slab)}$	=	$b_{(s)} \cdot E_{(s)} / E_{(b)}$	=	23.21	cm.	
n	=	E_s / E_c	=	6.81		

Uncracked Transformed Section

Similar to Model LS 1, centroid of area of uncracked section

Element	Area	y	Ay
Beam	30c	c/2	$15c^2$
Slab	185.68	c-21	185.68c-3899.28
Bar	49.47	c-19.5	49.47c-964.67
$\sum$			$15c^2$+235.15c-4863.95
	c	=	11.80 cm.

The moment of inertia of uncracked section :

Element	Area	y	I_g	Ay^2
Beam	354.00	5.90	4,108	12,323
Slab	185.68	- 9.20	990	15,716
Bar	49.47	- 7.70	-	2,933
$\sum$			5,098	30,972
I_{gt}		=	36,070	$cm.^4$

Cracked Transformed Section

Similar to Model LS 2, if the lower steel yield :

From equilibrium ; $C = T$

$$0.85f_c^{'}b\beta_1 c = A_s f_y$$

$$c = A_s f_y/(0.85f_c^{'}b\beta_1)$$

Substitute ; $\beta_1 = 0.85\text{-}0.05(f_c^{'}\text{-}280)/70$

$$= 0.77$$

Thus, neutral axis $c = 5.42$ cm.

Check whether $f_s = f_y$ i.e., the lower steel yield :

$$(\varepsilon_s + \varepsilon_{cu})/d = \varepsilon_{cu}/c$$

$$\varepsilon_s = \varepsilon_{cu}(d/c\text{-}1)$$

If $\varepsilon_s \geq \varepsilon_y$, then $f_s = f_y$

$$\varepsilon_y = f_y/E_s = 0.002$$

$$\varepsilon_s = 0.008 > \varepsilon_y$$

Thus, the section as being tension - controlled.

Therefore, from Appendix Figure D 6(b) and c able to obtain the moment of inertia of uncracked section, I_{cr} :

Element	Area	y	I_g	Ay^2
Beam	162.73	2.71	399	1,197
Bar	57.99	- 14.08	-	11,489
$\sum$			399	12,686
I_{cr}		=	13,085	cm.^{4}

1. Determine the Flexural Cracking Moment, M_{cr}

$$M_{cr} = f_r . I_g / y_t$$

$$f_r = 1.98\sqrt{f_c'}$$

= 39.30 ksc.

Thus ; M_{cr} = 1,074 kg.-m.

2. Determine the Nominal Moment Strength, M_n

M_n = T*(d-a/2)

= Asfy(d-a/2)

Thus ; M_n = 7,295 kg.-m.

3. Determine Load and Deflections due to M_{cr} & M_n

Similar to Model LS 1

M_{mid} = 0.5Pa

Δ_{mid} = $(P/2)L^3/ 6EI*(3a/4L-(a/L)^3)$

Therefore, load and deflection at cracking and yielding of Model LS 2

Point	Moment (kg.-m.)	P (kg.)	I ($cm.^4$)	Δ_{mid} (mm.)
Cracking	1,074	2,864	36,070	0.40
Yielding	7,295	19,453	13,085	7.56

Summary

The loads and deflections at points of cracking and yielding of the four specimens, as determined are shown

Appendix Table D1 Load and deflection at cracking and yielding points

Model	Point	Load (kg.)	Deflection (mm.)
MB 1	cracking	5,415	0.26
	yielding	37,514	3.80
LS 1	cracking	4,022	0.24
	yielding	35,853	3.77
MB 2	cracking	3,019	0.43
	yielding	19,508	7.94
LS 2	cracking	2,864	0.40
	yielding	19,453	7.56

The values in the table are used to plot load-deflection relationship for the four specimens in discussion, Figure 20.

Appendix E

Photographs of Experimental Work

Appendix Figure E1 Reinforcement preparation

Appendix Figure E2 Reinforcement preparation

Appendix Figure E3 Strain gauges attached to rebars

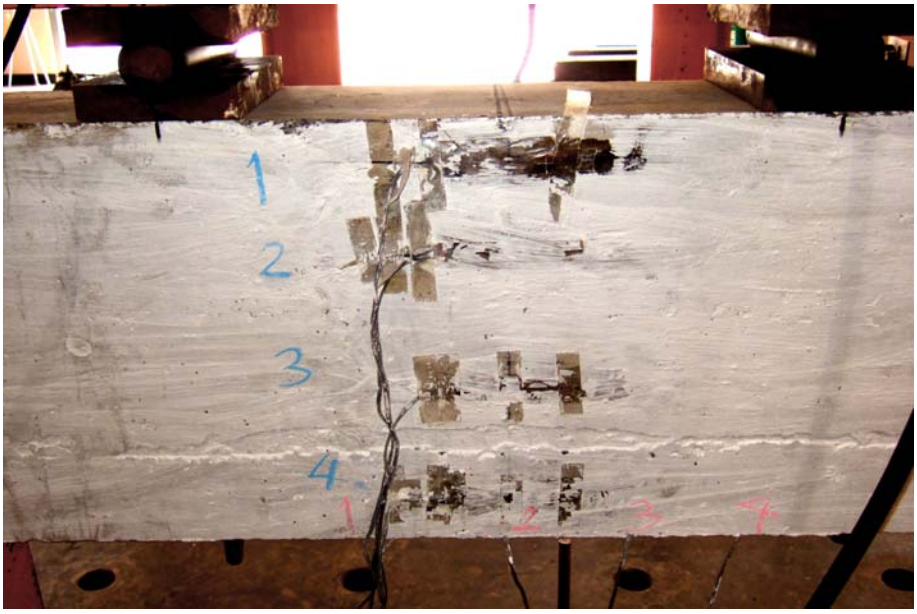

Appendix Figure E4 Strain gauges attached to concrete beam

Appendix Figure E5 Casting of precast beam

Appendix Figure E6 Casting of slab

Appendix Figure E7 Preparation of gap and non-shrinkage material

Appendix Figure E8 Joint of link-slab beam after filling non-shrinkage mortar

Appendix Figure E9 Frame for testing

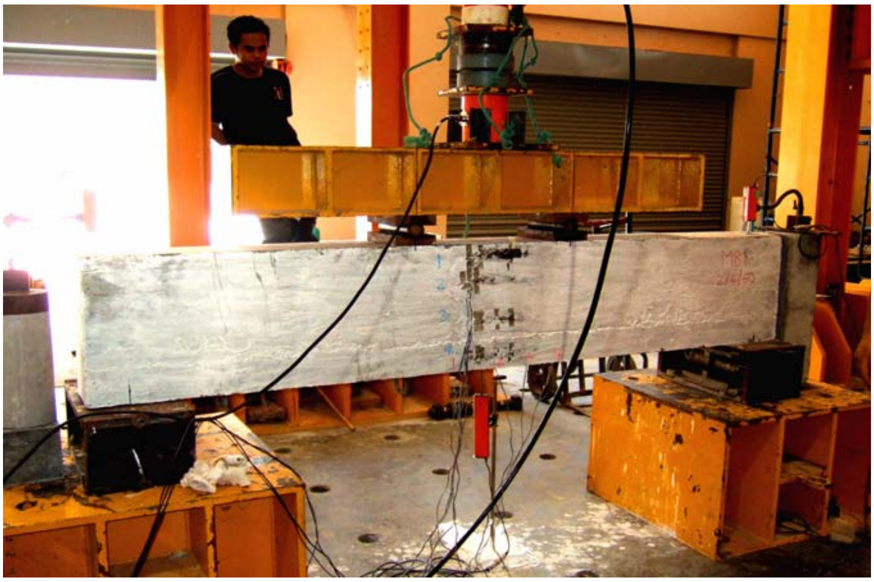

Appendix Figure E10 Set up specimen for testing

Appendix Figure E11 Cracking pattern on specimen model MB 1

Appendix Figure E12 Cracking pattern on specimen model LS 1

Appendix Figure E13 Cracking pattern on specimen model MB 2

Appendix Figure E14 Cracking pattern on specimen model LS1